Lattice Parton Collaboration

A Precise Determination of Collins-Soper Kernel from Lattice QCD

Jin-Xin Tan

Shanghai Jiao Tong University

Oct. 9 @LaMET 2025

In collaboration with:

Hang Liu, Zhi-Chao Gong, Qi-An Zhang, Wei Wang et.al

Outline

- ➢Motivation
- ➢Lattice QCD calculation of Collins-Soper Kernel
  - Quasi-TMD Wave Function
  - Collins-Soper Kernel
- ➢Summary and Outlook

Outline

- ➢Motivation
- ➢Lattice QCD calculation of Collins-Soper Kernel
  - Quasi-TMD Wave Function
  - Collins-Soper Kernel
- ➢Summary and Outlook

Exploration of Nucleon Structure

Gell-Mann quark model

Feynman parton model

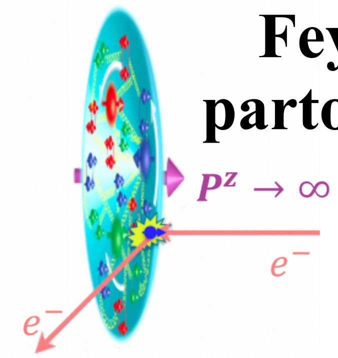

JLab
COMPASS
JAM
EIC
EicC
……

0D: spin and mass

1D: PDF

3D: TMDs

Higgs mechanism

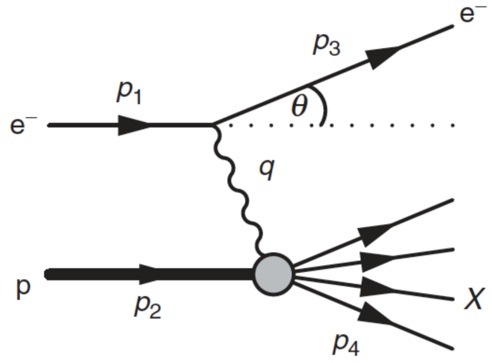

Deep inelastic scattering

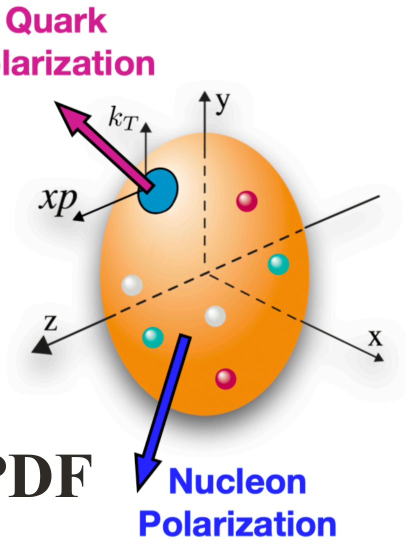

TMDPDF

Theoretical Complexity of TMDPDF -- Rapidity Divergence

➢ **Rapidity divergence from gluons radiation collinear to lightlike gauge link:**

$$I_{\rm div} \sim \int dk^+ dk^- \frac{f(k^+k^-)}{(k^+k^-)^{1+\varepsilon}} = \frac{1}{2}\int \frac{d(k^-/k^+)}{k^-/k^+} \int d(k^+k^-) \frac{f(k^+k^-)}{(k^+k^-)^{1+\varepsilon}}$$

$y_k = \frac{1}{2}\ln\frac{k^+}{k^-}$ $\quad y_k \to \pm\infty$: rapidity divergence

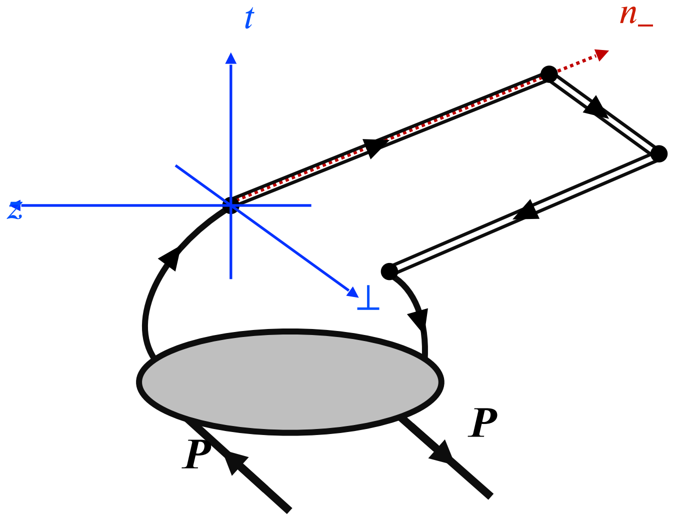

Rapidity divergence can be canceled by soft function,

leaving the rapidity scale ζ dependence $\sim e^{-\frac{1}{2}K(b_\perp,\mu)\ln\frac{\mu^2}{\zeta^2}}$

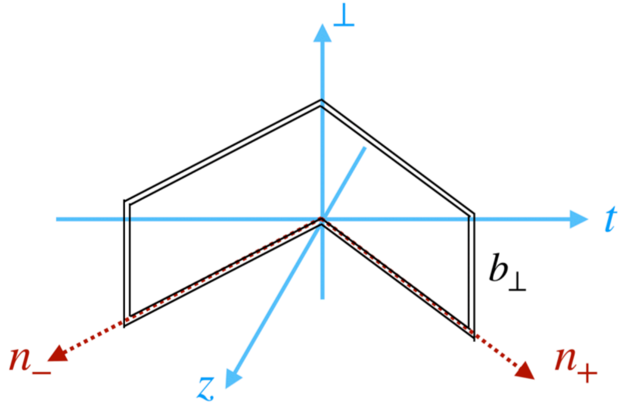

Ji et al., PRD 71, 034005(2005);
Collins, Vol. 32(Cambridge University Press, 2011).

Collins-Soper Kernel -- Describe Rapidity Evaluation of TMDs

- **Evolution of TMDs:**

$$f(x, b_\perp, \mu, \zeta) = f(x, b_\perp, \mu_0, \zeta_0)$$

$$\times \exp\left[\int_{\mu_0}^{\mu} \frac{d\mu'}{\mu'} \underline{\gamma_\mu(\mu', \zeta_0)}\right] \exp\left[\frac{1}{2} \underline{K(\mu, b_\perp)} \ln \frac{\zeta}{\zeta_0}\right]$$

UV anomalous dimension   **Rapidity anomalous dimension (Collins-Soper kernel)**

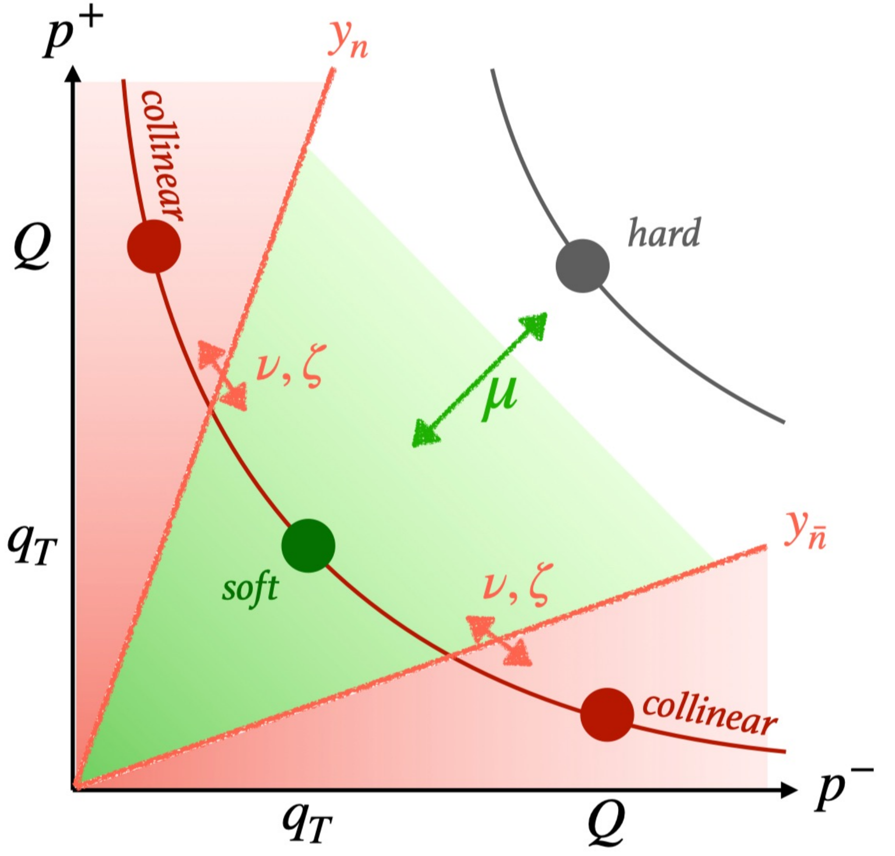

- **UV anomalous dimension γ_μ is perturbative (NLO, NNLO, …);**
- **Collins-Soper(CS) kernel $K(\mu, b_\perp)$ is nonperturbative for $b_\perp \gtrsim \Lambda_{\rm QCD}^{-1} \approx 0.2\text{fm}$.**

Ji et al., PRD 71, 034005(2005);
Collins, Vol. 32(Cambridge University Press, 2011).

CS Kernel -- An Essential Component for Lattice Calculations of TMDs

➢ **LaMET framework:** *Ji, PRL 110, 262002 (2013); Ji, Sci.China 57 (2014)*

Matching kernel

$$\tilde{f}_{\Gamma}(x, b_{\perp}, \mu, \zeta^z) S_I^{\frac{1}{2}}(b_{\perp}, \mu) = H_{\Gamma}(\zeta^z, \mu) \exp\left[\frac{1}{2} K(b_{\perp}, \mu) \ln \frac{\zeta^z - i\epsilon}{\zeta}\right] f(x, b_{\perp}, \mu, \zeta) + \mathcal{O}\left(\frac{\Lambda_{\text{QCD}}^2}{\zeta^z}, \frac{M^2}{(P^z)^2}, \frac{1}{b_{\perp}^2 \zeta^z}\right)$$

Quasi TMDs **Intrinsic soft function** **Collins-Soper kernel** **Light-cone TMDs**

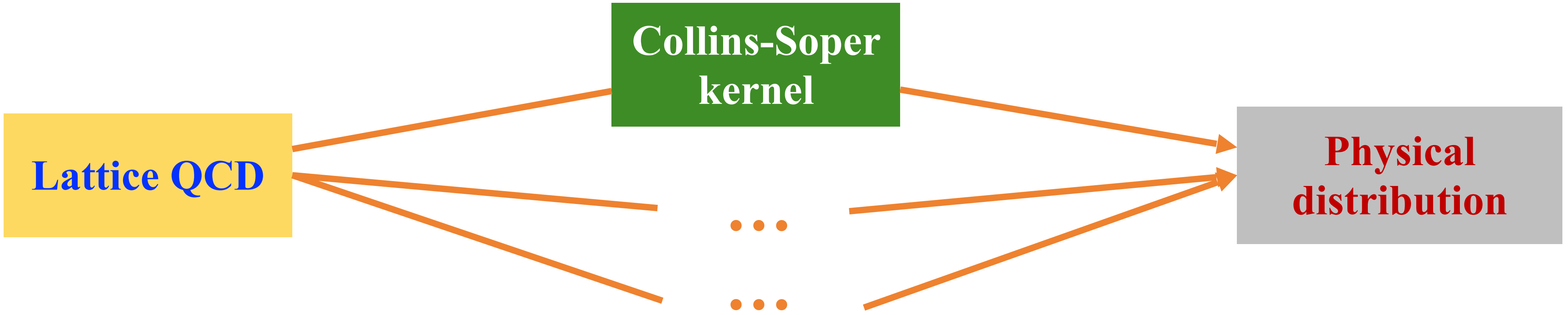

Ji et al., PLB811(2020);
Ebert et al., JHEP 09 (2019);
Ebert et al., JHEP04(2022);

Outline

➢Motivation

➢Lattice QCD calculation of Collins-Soper Kernel

- **Quasi-TMD Wave Function**
- Collins-Soper Kernel

➢Summary and Outlook

From quasi TMDs to Collins-Soper kernel

- **At leading power accuracy, CS kernel can be extracted from the P^z dependence of TMDs:**

Matching kernel

$$\tilde{f}_\Gamma(x, b_\perp, \mu, \zeta^z) S_I^{\frac{1}{2}}(b_\perp, \mu) = H_\Gamma(\zeta^z, \mu) \exp\left[\frac{1}{2} K(b_\perp, \mu) \ln \frac{\zeta^z - i\epsilon}{\zeta}\right] f(x, b_\perp, \mu, \zeta) + \mathcal{O}\left(\frac{\Lambda_{\rm QCD}^2}{\zeta^z}, \frac{M^2}{(P^z)^2}, \frac{1}{b_\perp^2 \zeta^z}\right)$$

Quasi TMDs   Intrinsic soft function   Collins-Soper kernel   Light-cone TMDs

Taking ratio, S_I and f cancelled each other, then

$$K(b_\perp, \mu) = \frac{1}{\ln(P_1^z / P_2^z)} \ln\left(\frac{H_\Gamma(\zeta_2^z, \mu) \tilde{f}_\Gamma(x, b_\perp, \zeta_1^z, \mu)}{H_\Gamma(\zeta_1^z, \mu) \tilde{f}_\Gamma(x, b_\perp, \zeta_2^z, \mu)}\right)$$

$\tilde{f}_\Gamma$ could be either unsubtracted quasi TMD wave function or quasi TMDPDF.

Ji, PRL 110, 262002 (2013);
Ji, Sci.China 57 (2014)

From quasi TMDs to Collins-Soper kernel

- ➢ **At leading power accuracy, CS kernel can be extracted from the P^z dependence of TMDs:**

Bollweg et al.,PLB852, 138617 (2024); Walter, et al.(LPC),PRD.111.094507(2024).

Matching kernel

Quas

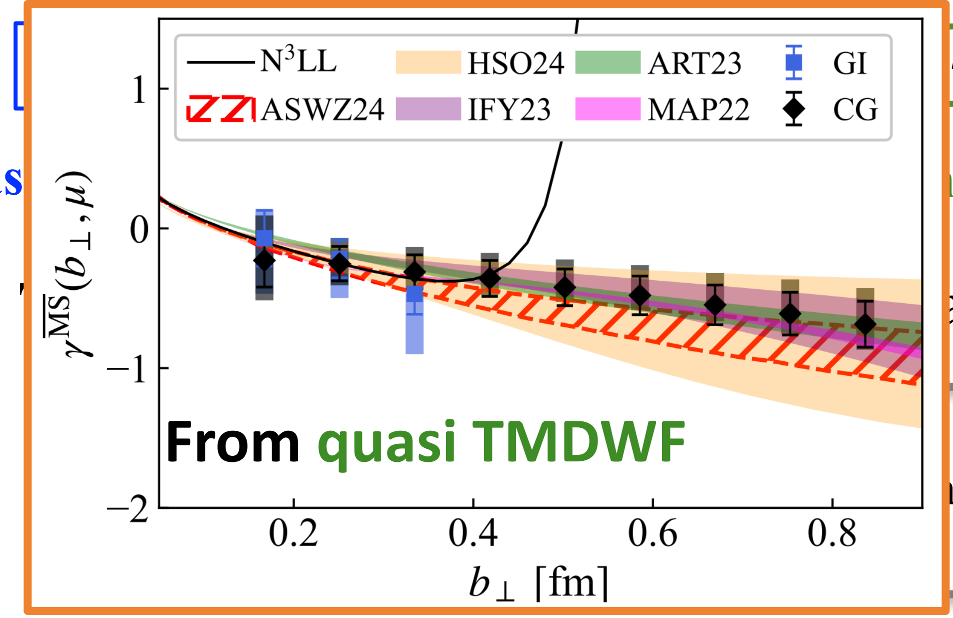

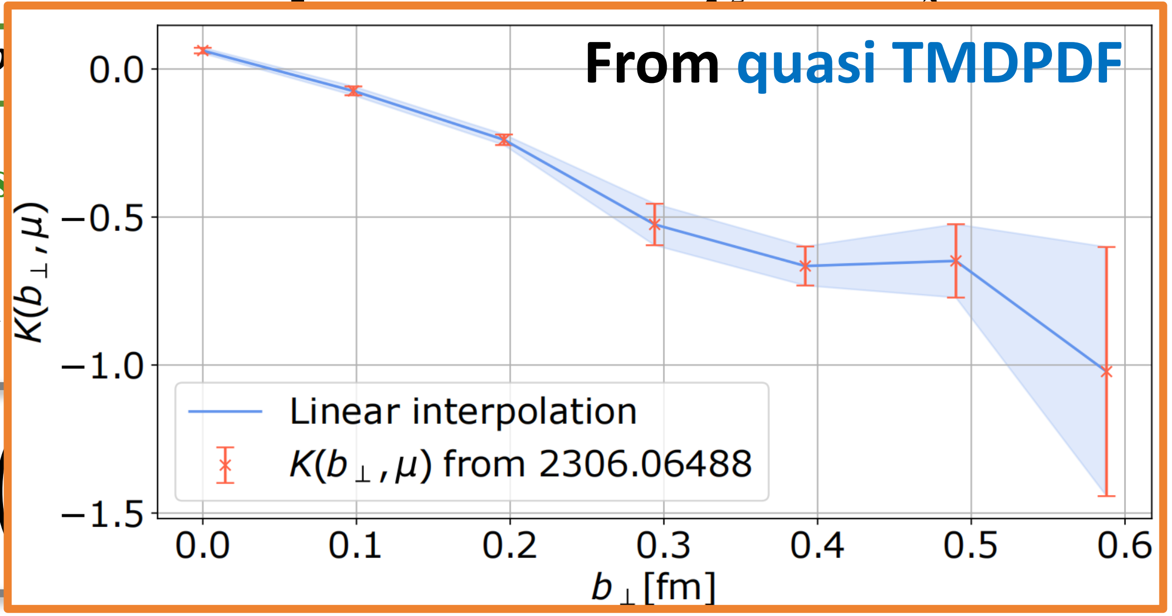

$\tilde{f}_\Gamma$ **could be either unsubtracted quasi TMD wave function or quasi TMDPDF.**

For better signal, the CS kernel is extracted from the pion quasi-TMDWF.

Quasi TMD Wave Function

- **The quasi-TMD wave functions can be defined as:**

$$\tilde{\Psi}^{\pm}(x, b_\perp, \mu, \zeta_z) = \lim_{L\to\infty} \int \frac{dzP^z}{2\pi} e^{ixzP^z} \frac{\tilde{\Phi}^{\pm 0}(z, b_\perp, P^z, a, L)}{Z_O(\mu, a)\sqrt{Z_E(2L+z, b_\perp, \mu, a)}},$$

where the bare quasi-TMD wave function can be constructed as :

$$\tilde{\Phi}^{\pm 0}(z, b_\perp, P^z, a, L) = \left\langle 0 \,|\, \bar{q}(z\hat{n}_z + b_\perp \hat{n}_\perp) \Gamma U_{\sqsupset,\pm}(L, z, b_\perp) q(0) \,|\, P^z \right\rangle.$$

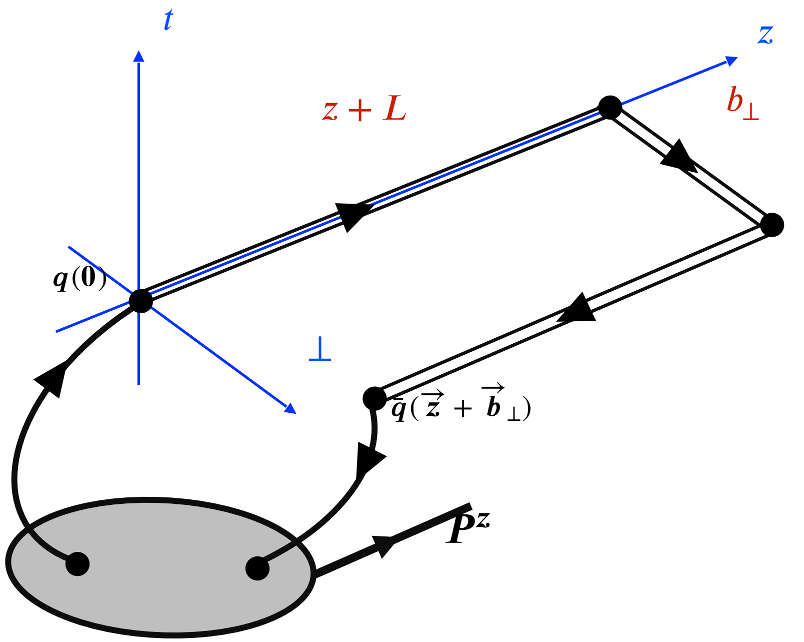

Chu et al.(LPC), PRD109(2024);
Chu et al.(LPC), PRD 106(2022);
Zhang et al., PRL125(2020).

Lattice Setup

- ➢ **CLQCD lattice ensembles with multiple lattice spacings and physical pion masses;**
- ➢ **Coulomb gauge fixed wall source propagators;**
- ➢ **HYP smearing.**

	a/fm	/MeV	/GeV
C32P29	0.10530	292.4	1.47, 1.84, 2,21
C32P23	0.10530	228.0	1.47, 1.84, 2,21
C48P14	0.10530	135.5	0.98, 1.22, 1.47
F32P30	0.07746	303.2	2.00, 2.50, 3.00
H48P32	0.05187	317.2	1.99, 2.59, 2.99

Hu et al.(CLQCD), PRD 109 (2024); Hasenfratz et al., PRD 64, 034504(2001).

Extract Bare Quasi-TMDWF Matrix Elements

- **To determine the bare quasi-TMDWF, we construct the non-local two point correlation function :**

$$C_2^{\pm}(z, b_\perp, P, p^z, L, t, t') = \frac{1}{n_s^3} \sum_{\vec{x}} e^{i\vec{P}\cdot\vec{x}} \mathrm{Tr}\langle S_w(t'; \vec{x} + L\hat{n}_z + b\hat{n}_x, t; -p^z) \times U_{\sqsupset,\pm}(L, z, b_\perp) \Gamma_1 S_w(\vec{x} + L\hat{n}_z + z\hat{n}_z, t; t'; p^z) \Gamma_2 \rangle$$

- **The bare matrix elements can be extracted by one-/two-state fit:**

$$R^{\pm}(z, b_\perp, P^z, L, t) = \frac{C_2^{\pm}(z, b_\perp, P^z, L, t)}{C_2(0, 0, P^z, 0, t)} = \tilde{\Phi}^{\pm 0}(z, b_\perp, P^z, L) e^{-iz\frac{P^z}{2}} \times \left[1 + c_1(z, b_\perp, P^z, L) e^{-\Delta E t}\right]$$

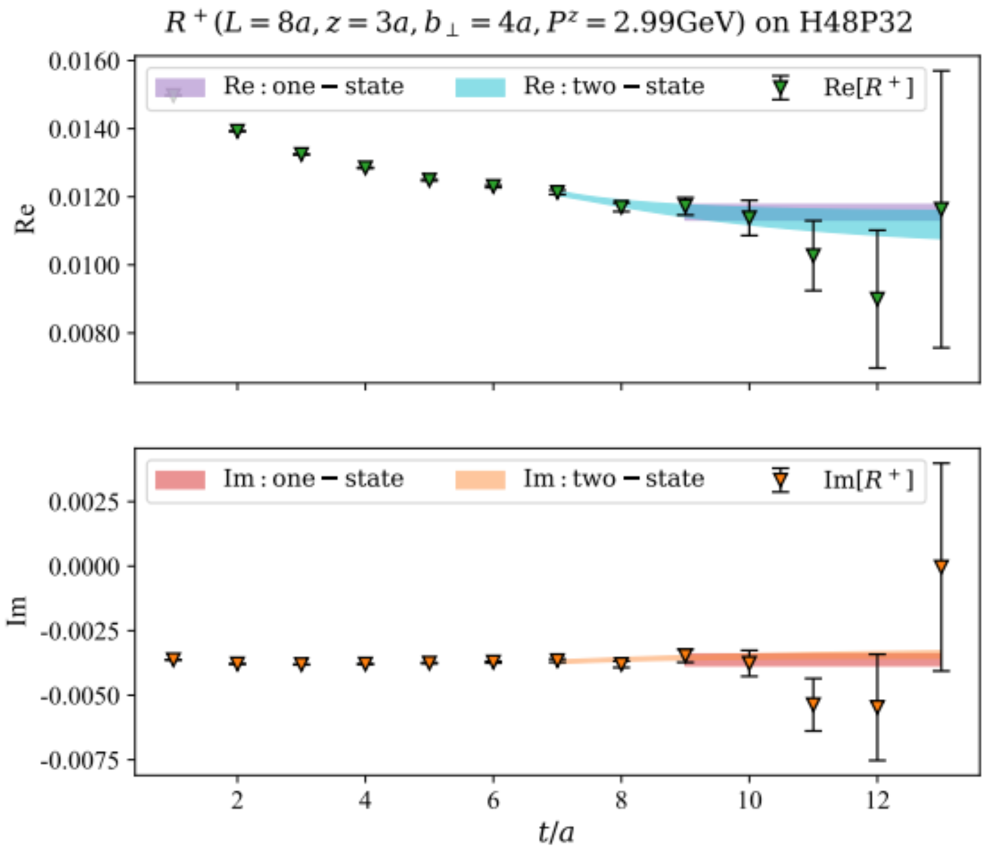

LPC, in preparation

Wilson Loop Renormalization of Bare Quasi-TMDWFs

- **Wilson loop definition:**

Ji et al., PRL120(11):112001, 2018.

$Z_E =$

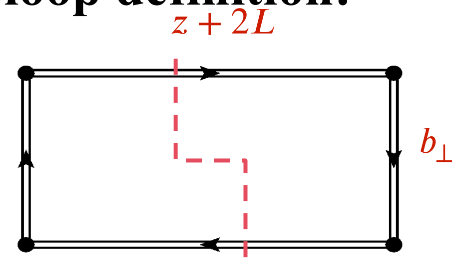

$$Z_E(2L+z, b_\perp) = \frac{1}{N_c} Tr \left\langle 0 \,|\, U_\perp\left(0; b_\perp \hat{n}_\perp\right) U_z\left(b_\perp \hat{n}_\perp; (2L+z)\hat{n}_z\right) |\, 0 \right\rangle$$

- **Parameterization:**

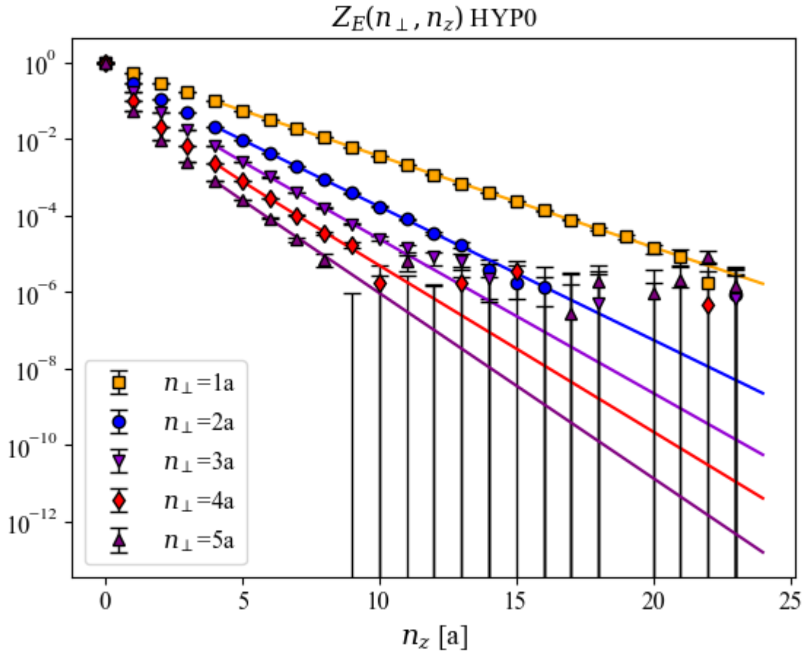

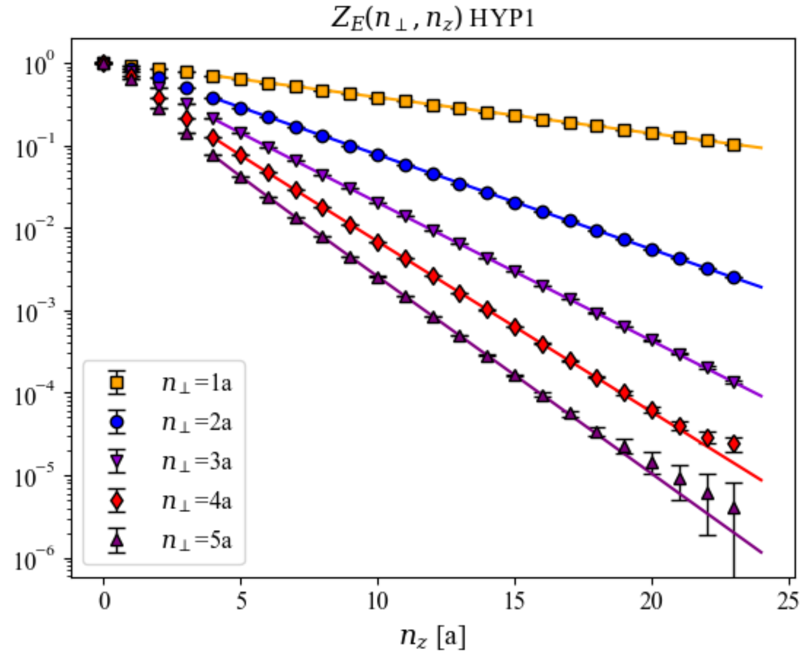

LPC, in preparation

Self-Renormalization--a New Scheme to Extract Z_O

Subtracted matrix element

- **Renormalization condition:** $\tilde{h}(a,z,b_\perp) = \frac{\tilde{\Phi}^0(z,b,Pz=0,\mu)}{\sqrt{Z_E(z+2L,b,\mu)}} = Z_O(1/a,\mu)h_0^{\overline{MS}}(\mu,b_\perp,z) + O(\frac{a^2}{b^2})$
- **Parametrization:**

$$\ln \tilde{h}(a,z,b_\perp) = \frac{\gamma_0}{\beta_0}\ln\left[\ln[1/(a\Lambda_{QCD})]\right] + \frac{c_1}{\ln[1/(a\Lambda_{QCD})]} + g(z,b_\perp)$$

Joint fit result: c_1=0.020

$$\ln Z_O(a,\mu) = \frac{\gamma_0}{\beta_0}\ln\left[\ln[1/(a\Lambda_{QCD})]\right] + \frac{c_1}{\ln[1/(a\Lambda_{QCD})]} + d'(\mu)$$

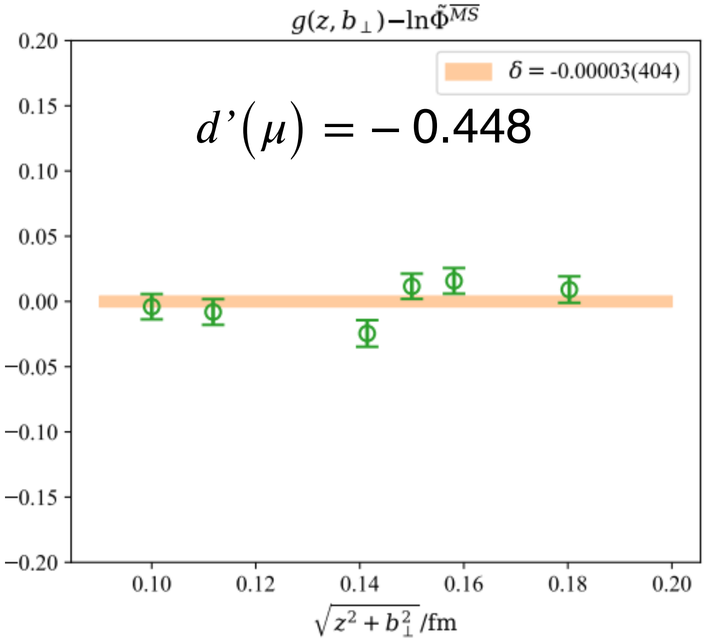

LPC, in preparation

fm	0.10530	0.07746	0.05187
HYP0	1.064(21)	1.145(20)	1.241(19)
HYP1	0.92208(62)	0.97526(57)	1.03969(53)

For more details, please see Hao-Yang and Mu-Hua's talks.

Deng et al., JHEP 09 (2022); Huo et al. NPB 969(2021)

Result for Quasi-TMDWFs in Coordinate Space

Different HYP steps

$$\tilde{\Phi}^{\pm}(z, P^z, L, b, \mu) = \frac{\tilde{\Phi}^{\pm 0}(z, b_\perp, P^z, a, L)}{Z_O(\mu, a)\sqrt{Z_E(2L + z, b_\perp, \mu, a)}}$$

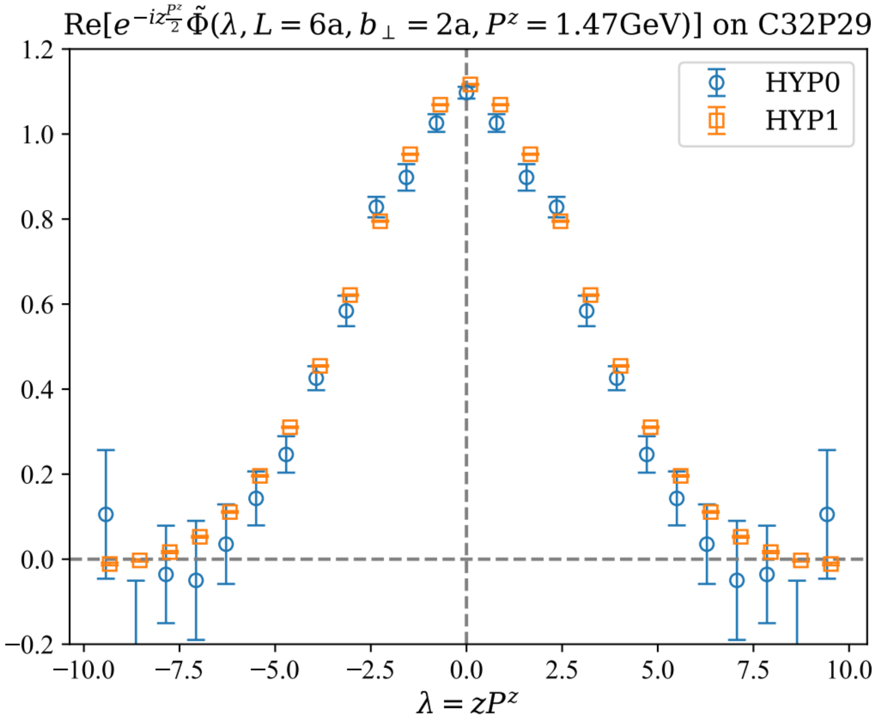

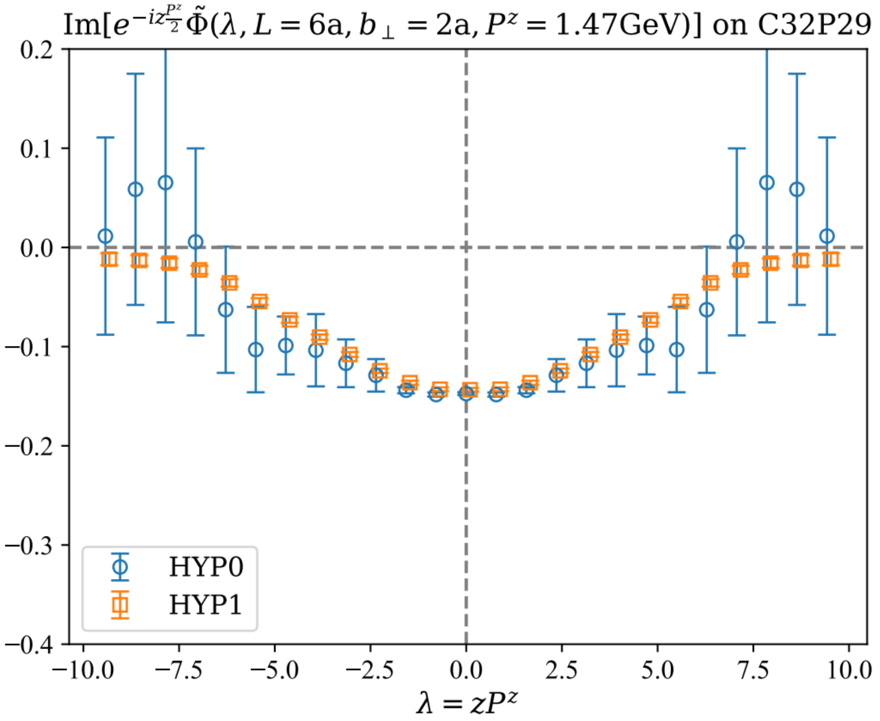

LPC, in preparation

Result for Quasi-TMDWFs in Coordinate Space

$$\tilde{\Phi}^{\pm}(z, P^z, L, b, \mu) = \frac{\tilde{\Phi}^{\pm 0}(z, b_\perp, P^z, a, L)}{Z_O(\mu, a)\sqrt{Z_E(2L+z, b_\perp, \mu, a)}}$$

Different P^z

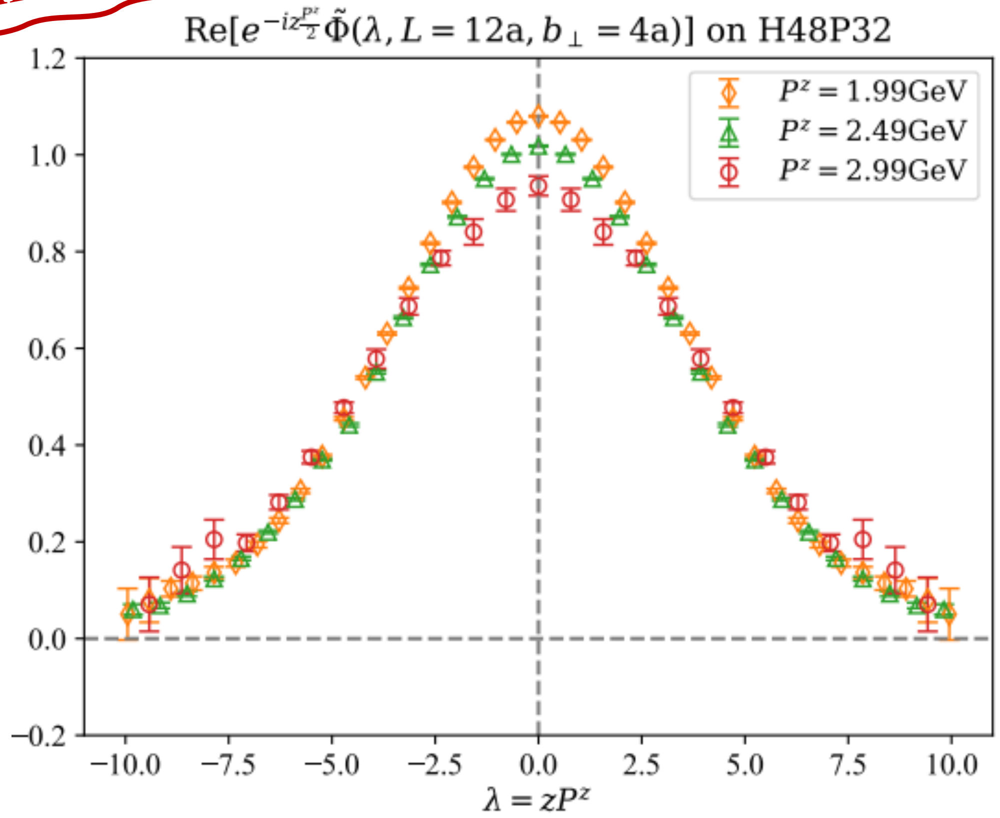

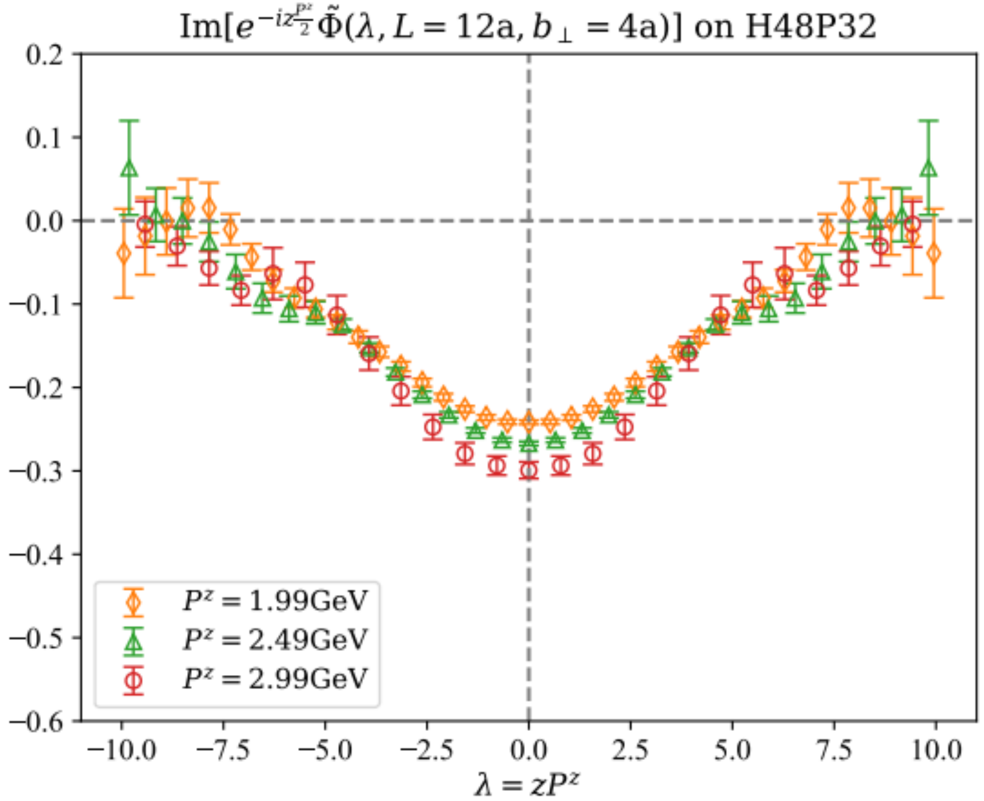

LPC, in preparation

Result for Quasi-TMDWFs in Coordinate Space

$$\tilde{\Phi}^{\pm}(z, P^z, L, b, \mu) = \frac{\tilde{\Phi}^{\pm 0}(z, b_\perp, P^z, a, L)}{Z_O(\mu, a)\sqrt{Z_E(2L + z, b_\perp, \mu, a)}}$$

Different $b_\perp$

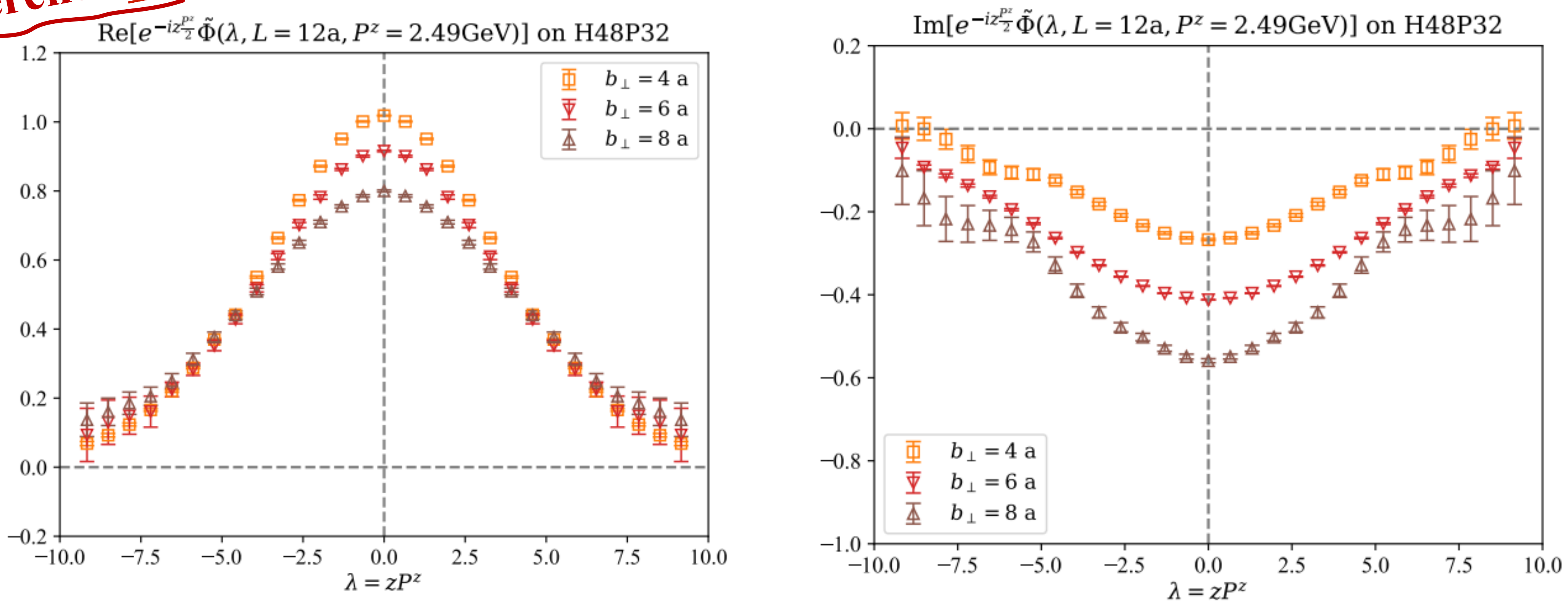

LPC, in preparation

Extrapolation for Large λ

➢ **In large λ area, a feasible form of asymptotic behavior can be written as:**

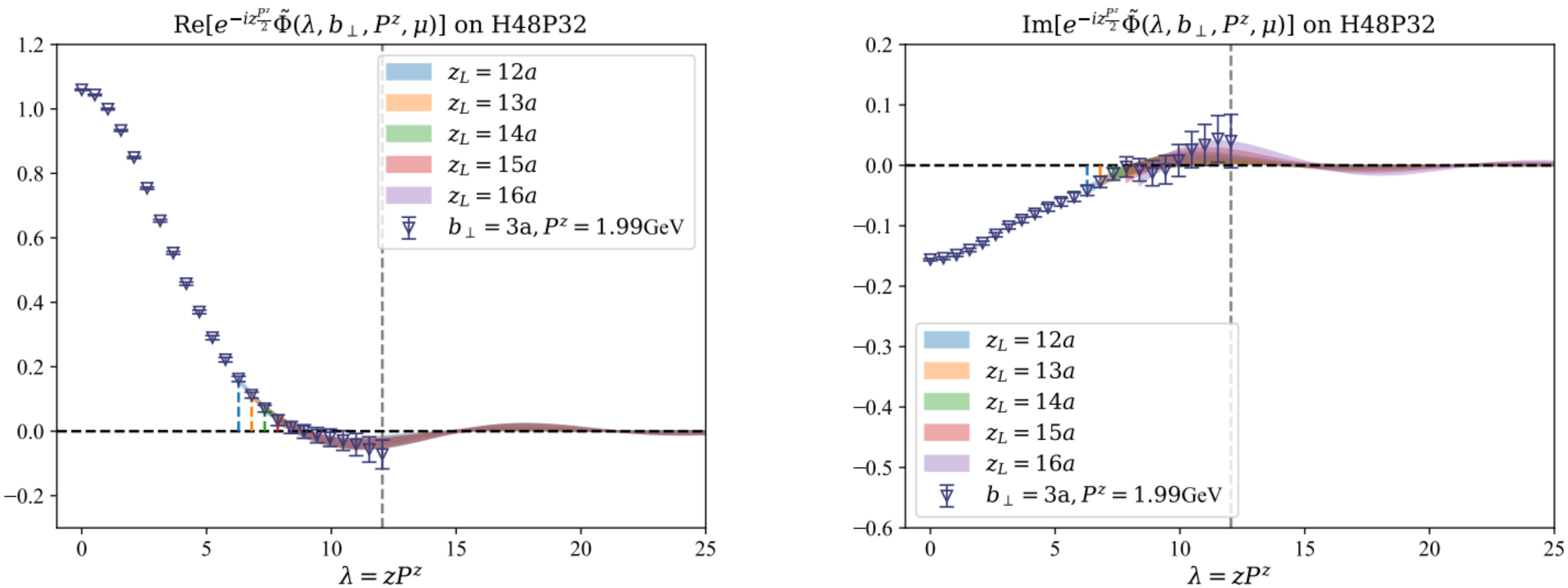

LPC, in preparation

Result for Quasi-TMDWFs in Momentum Space

$$\tilde{\Psi}^{\pm}(x, b_\perp, \mu, \zeta_z) = \lim_{L\to\infty} \int \frac{dz}{2\pi} e^{ixzP^z} \tilde{\Phi}^{\pm}(z, P^z, L, b, \mu)$$

Different HYP steps

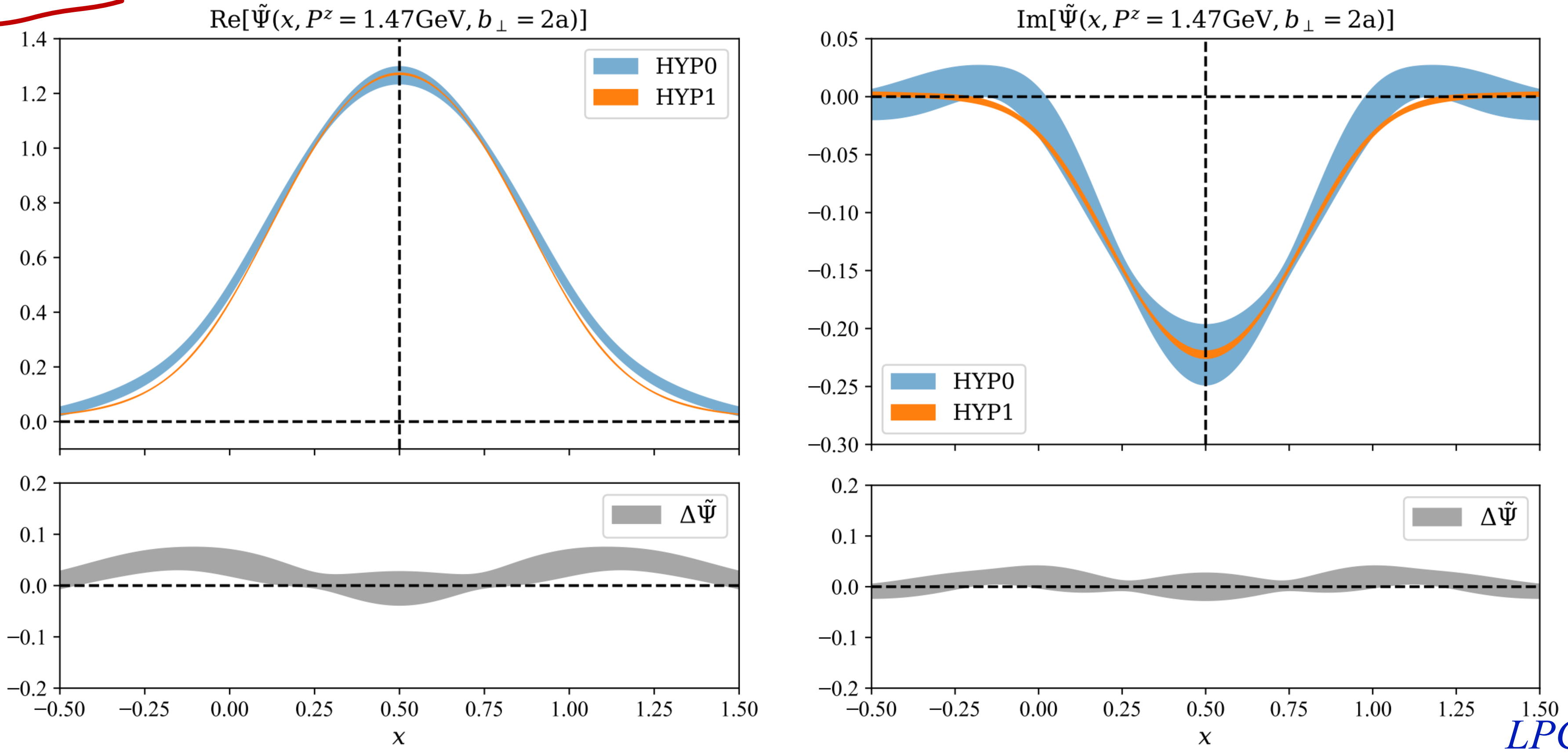

LPC, in preparation

Result for Quasi-TMDWFs in Momentum Space

$$\tilde{\Psi}^{\pm}(x, b_\perp, \mu, \zeta_z) = \lim_{L\to\infty} \int \frac{dz}{2\pi} e^{ixzP^z} \tilde{\Phi}^{\pm}(z, P^z, L, b, \mu)$$

Different HYP steps

HYP smearing:
- ✓ Better signal;
- ✓ Same physics.

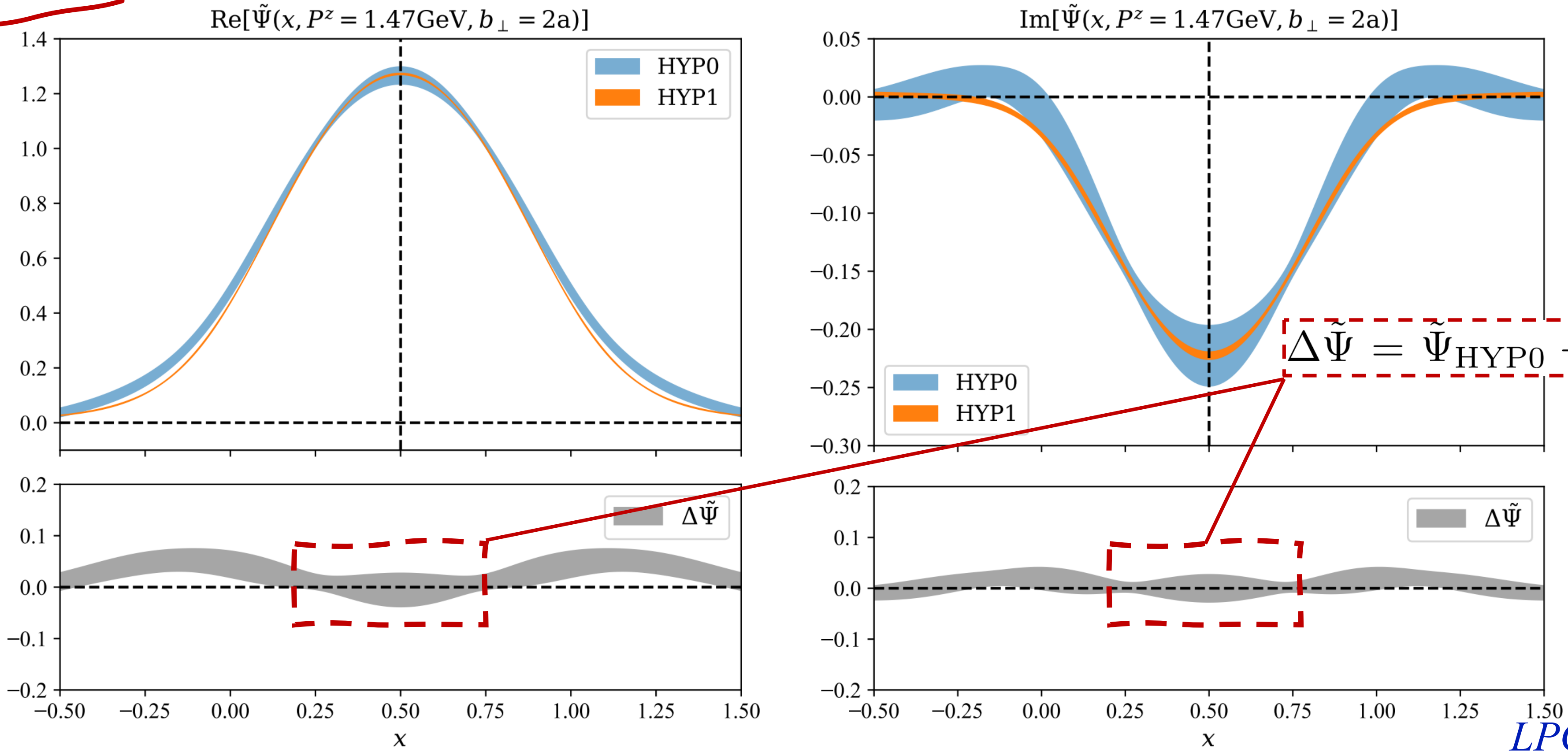

$\Delta\tilde{\Psi} = \tilde{\Psi}_{\mathrm{HYP0}} - \tilde{\Psi}_{\mathrm{HYP1}}$ (gray)

LPC, in preparation

Result for Quasi-TMDWFs in Momentum Space

$$\tilde{\Psi}^{\pm}(x, b_\perp, \mu, \zeta_z) = \lim_{L\to\infty} \int \frac{dz}{2\pi} e^{ixzP^z} \tilde{\Phi}^{\pm}(z, P^z, L, b, \mu)$$

Different P^z

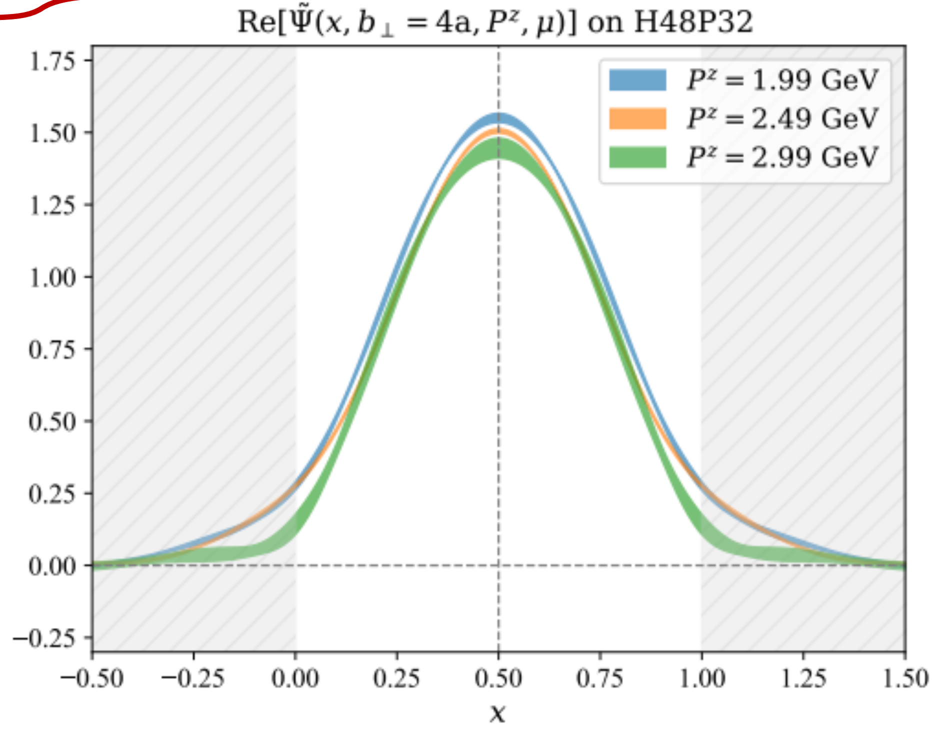

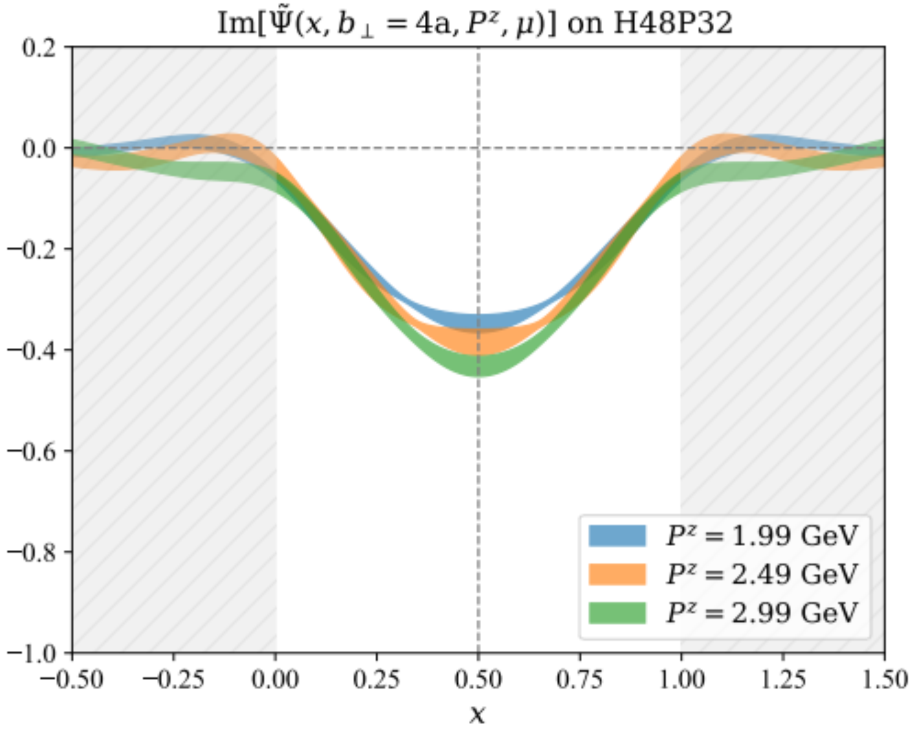

LPC, in preparation

Result for Quasi-TMDWFs in Momentum Space

$$\tilde{\Psi}^{\pm}(x, b_\perp, \mu, \zeta_z) = \lim_{L\to\infty} \int \frac{dz}{2\pi} e^{ixzP^z} \tilde{\Phi}^{\pm}(z, P^z, L, b, \mu)$$

Different $b_\perp$

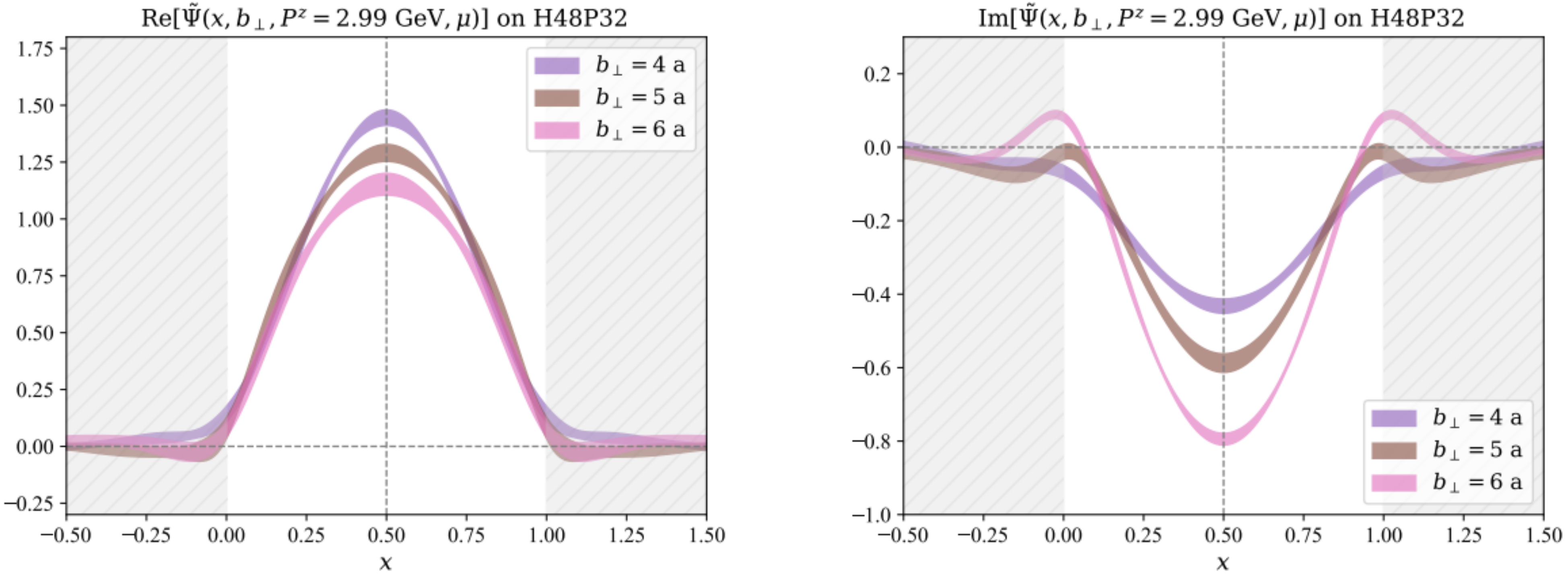

LPC, in preparation

Outline

- ➢Motivation
- ➢Lattice QCD calculation of Collins-Soper Kernel
  - Quasi-TMD Wave Function
  - Collins-Soper Kernel
- ➢Summary and Outlook

CS Kernel Extracted from Quasi-TMDWFs

quasi-TMDWFs

$$K(b_\perp, \mu; a, x, P_1^z, P_2^z) = \frac{1}{\ln(P_1^z/P_2^z)} \ln\left(\frac{h(xP_2^z, \mu)\tilde{\Psi}^{\pm}(x, b_\perp, \mu, P_1^z)}{h(xP_1^z, \mu)\tilde{\Psi}^{\pm}(x, b_\perp, \mu, P_2^z)}\right)$$

matching kernel

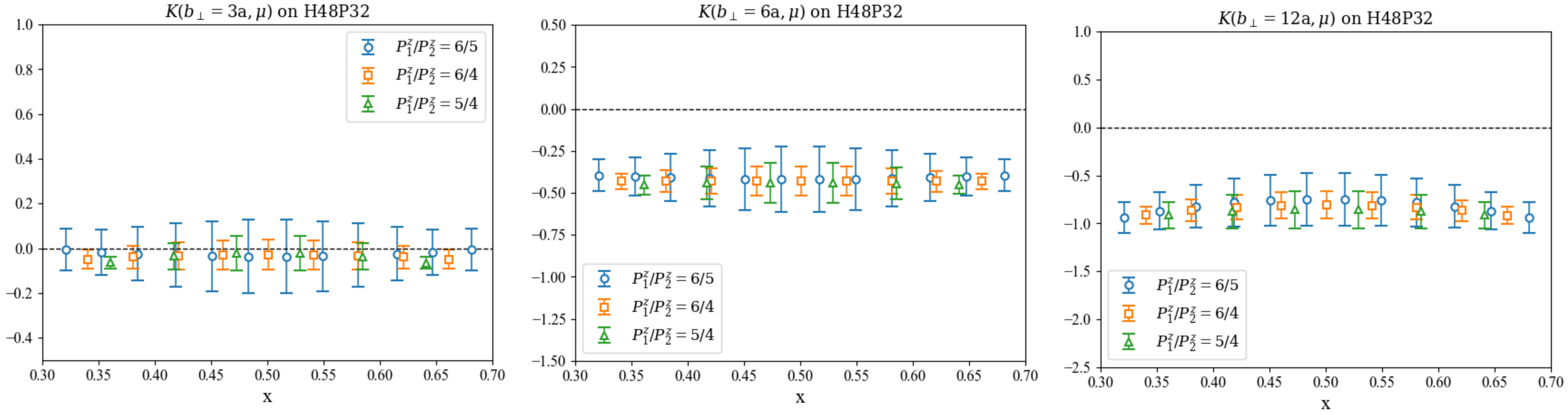

(For better visualization, we present a subset of points selected from the 200 data points in each of the 3 cases.)

LPC, in preparation

Avkhadiev, et al., PRD 108, 114505 (2023).

Large Momentum Limit Extrapolation

$$K(b_\perp, \mu; a, x, P_1^z, P_2^z) = K(b_\perp, \mu; a) + \left[\frac{1}{(P_1^z)^2} - \frac{1}{(P_2^z)^2}\right] \frac{1}{x^2(1-x)^2} A(b_\perp, x, \mu; a)$$

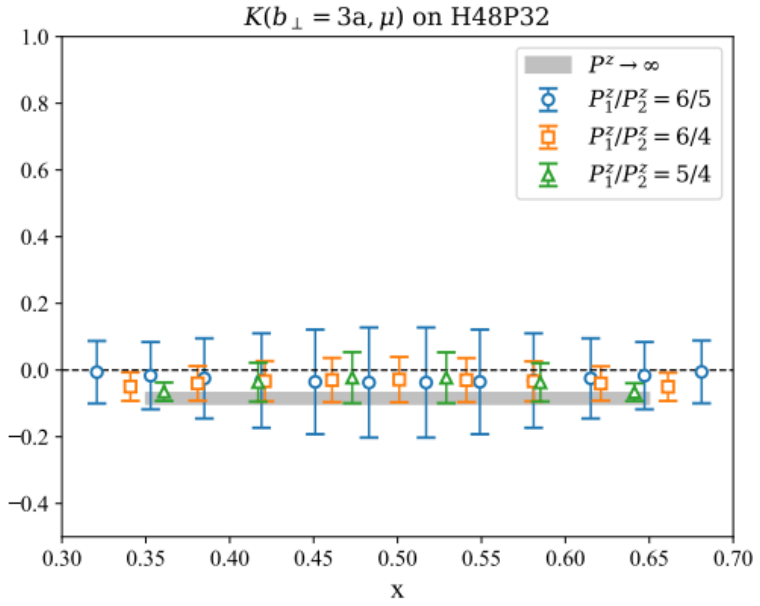

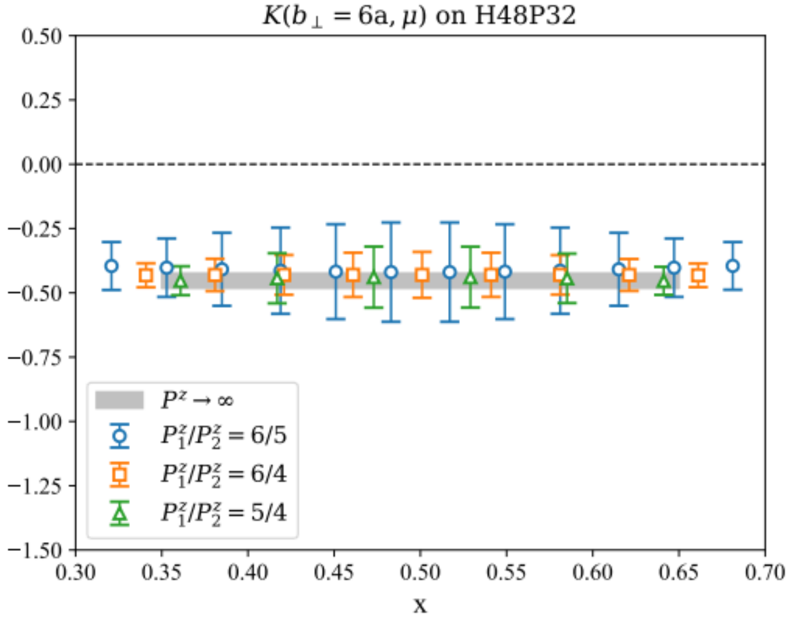

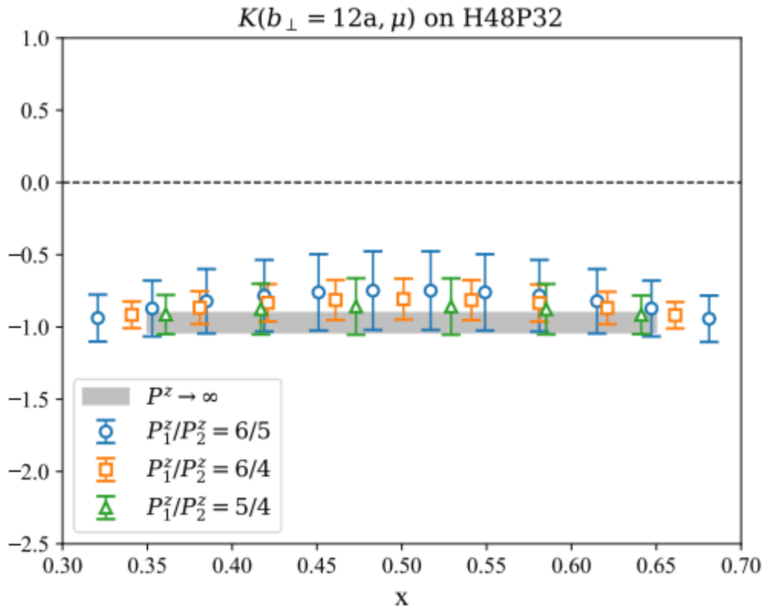

(For better visualization, we present a subset of points selected from the 200 data points in each of the 3 cases.)

LPC, in preparation

Large Momentum Limit Extrapolation

$$K(b_\perp,\mu;a,x,P_1^z,P_2^z) = K(b_\perp,\mu;a) + \left[\frac{1}{(P_1^z)^2} - \frac{1}{(P_2^z)^2}\right]\frac{1}{x^2(1-x)^2}A(b_\perp,x,\mu;a)$$

... repeat for each $b_\perp$ and each ensemble ...

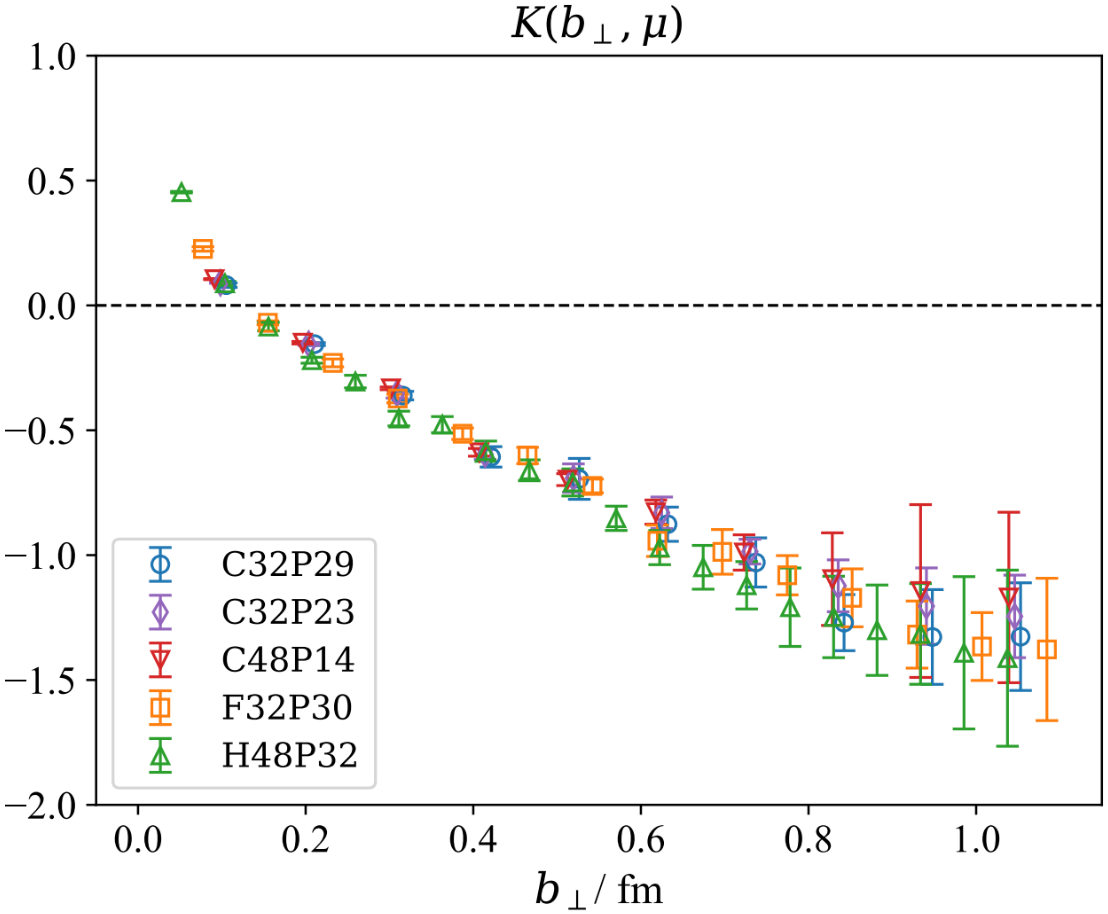

LPC, in preparation

Continuum Limit and Physical Mass Extrapolation

$$K(b_\perp, \mu; a, m_\pi) = K(b_\perp, \mu) + a^2 B(b_\perp, \mu) + (m_\pi^2 - m_{\pi,phy}^2) C(b_\perp, \mu)$$

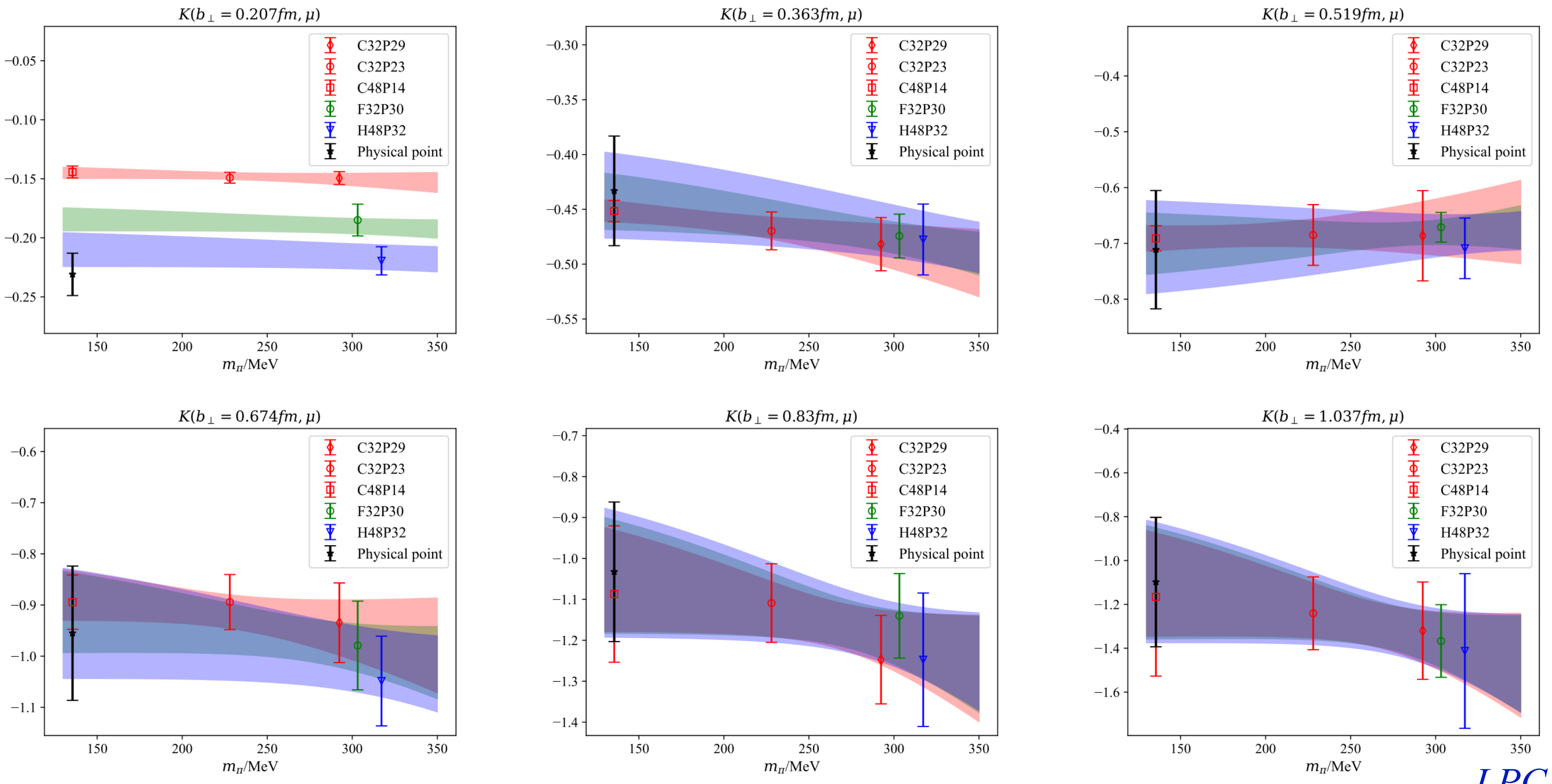

LPC, in preparation

The Systematic Uncertainty

➢ **We have considered four sources of systematic uncertainties:**

1.the unphysical imaginary part,

2.the large-λ extrapolation,

3.the large-momentum extrapolation,

4.the continuum and physical mass extrapolations.

"Imaginary part" of the CS kernel

➢ **Systematic uncertainty from the imaginary part of the CS kernel:**

$$\sigma_{\text{sys}}^{\text{Im}} = \sqrt{K(b_\perp,\mu)^2 + \text{Im}[K(b_\perp,\mu)^2]} - |K(b_\perp,\mu)|$$

➢ **Previous studies have shown that the imaginary part of the CS kernel primarily originates from the matching kernel.**

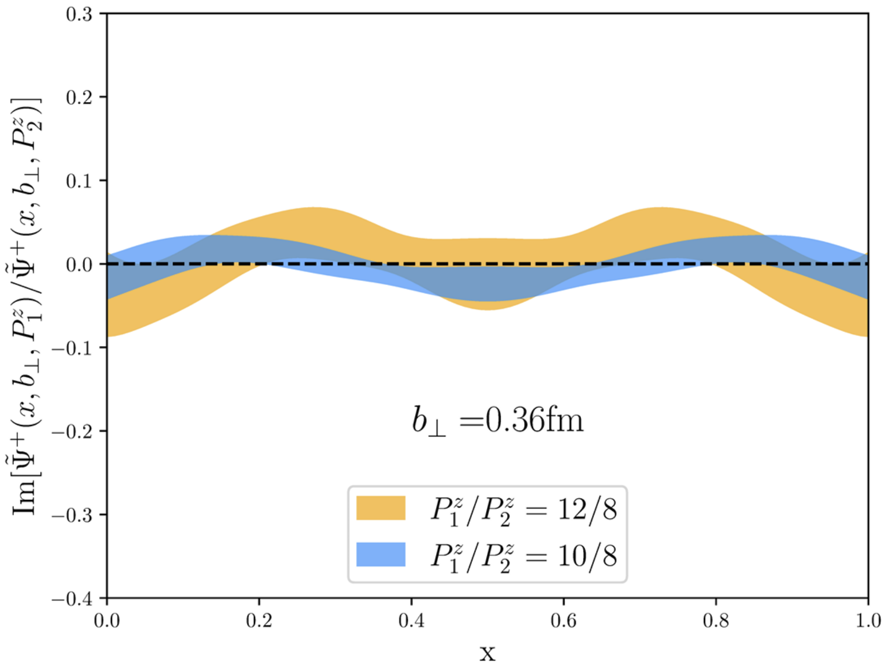

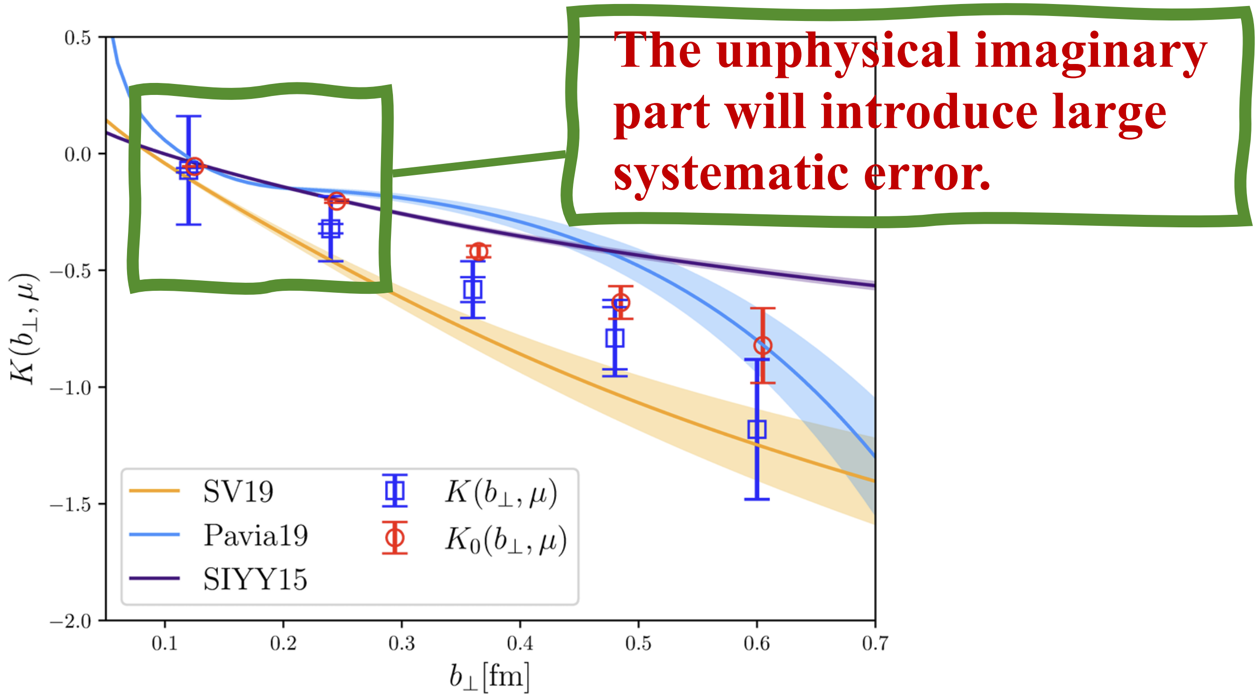

Chu et al. (LPC), PRD 106, 034509 (2022);

"Imaginary part" of the CS kernel

➢ The quasi-TMDWF factorization formula requires $xP^z b_\perp \gg 1$, at small $b_\perp$ region, remain the **dependence on $b_\perp$** when computing the matching kernel.

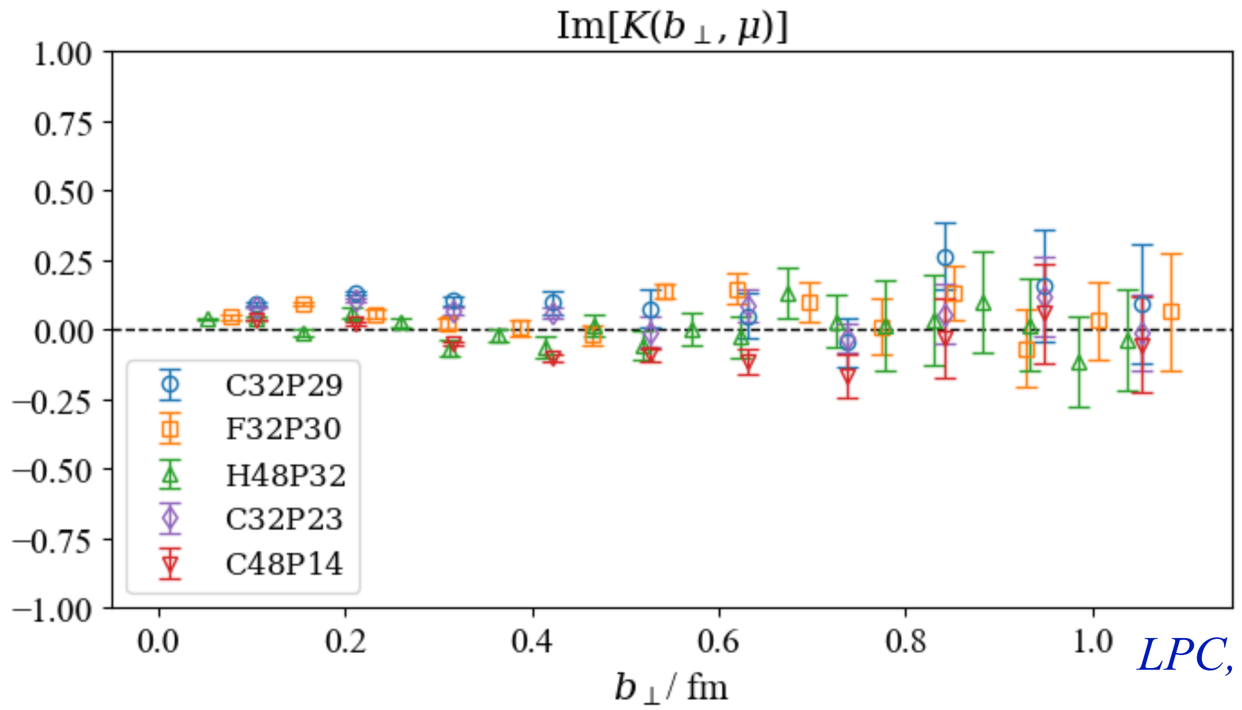

LPC, in preparation

Imaginary parts of the CS kernel are all very close to zero!

Avkhadiev, et al., PRD 108, 114505 (2023).

The Systematic Uncertainty

- ➢ **We have considered four sources of systematic uncertainties:**

1.the unphysical imaginary part, **2.the large-λ extrapolation,**
3.the large-momentum extrapolation, **4.the continuum and physical mass extrapolations.**

- ➢ **For these extrapolations(2, 3, 4), the difference of the result with different extrapolation schemes denotes the systematic error.**

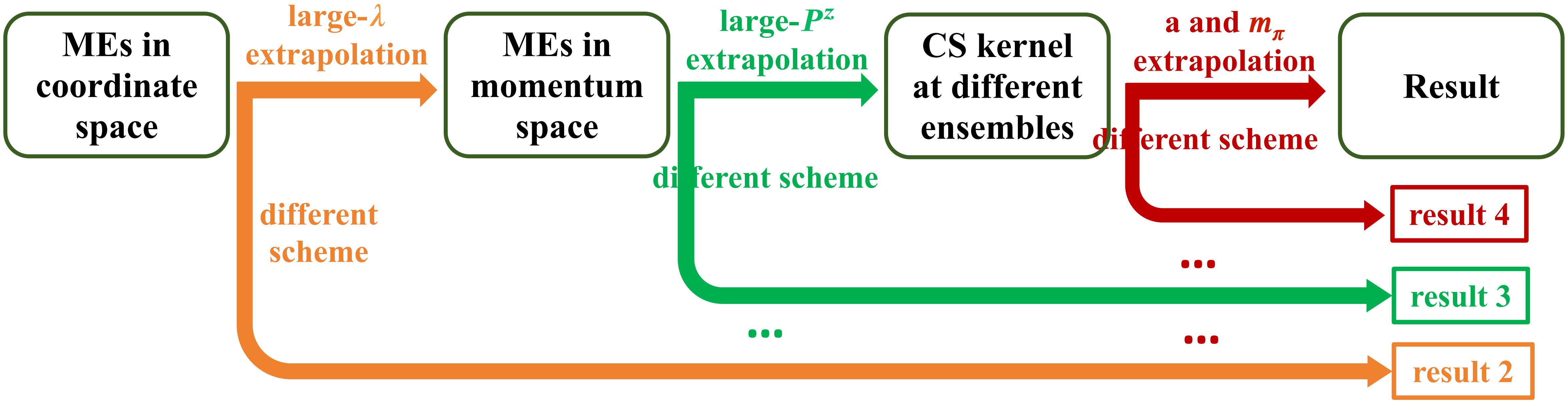

The Systematic Uncertainty

➢ **We have considered four sources of systematic uncertainties:**

1.the unphysical imaginary part, **2.the large-λ extrapolation,**

3.the large-momentum extrapolation, **4.the continuum and physical mass extrapolations.**

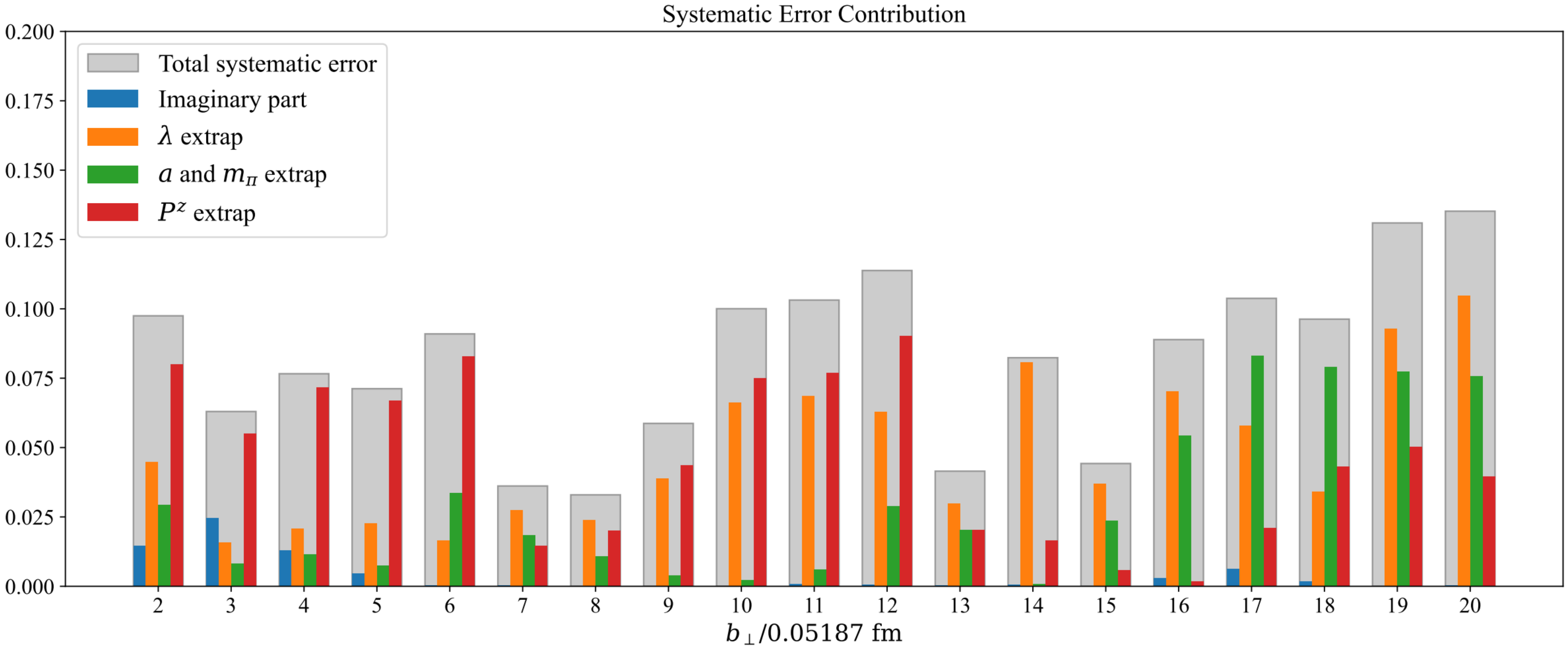

Final Result

✓ Continuum ✓ Physical ✓ $b_\perp = 1\text{fm.}$

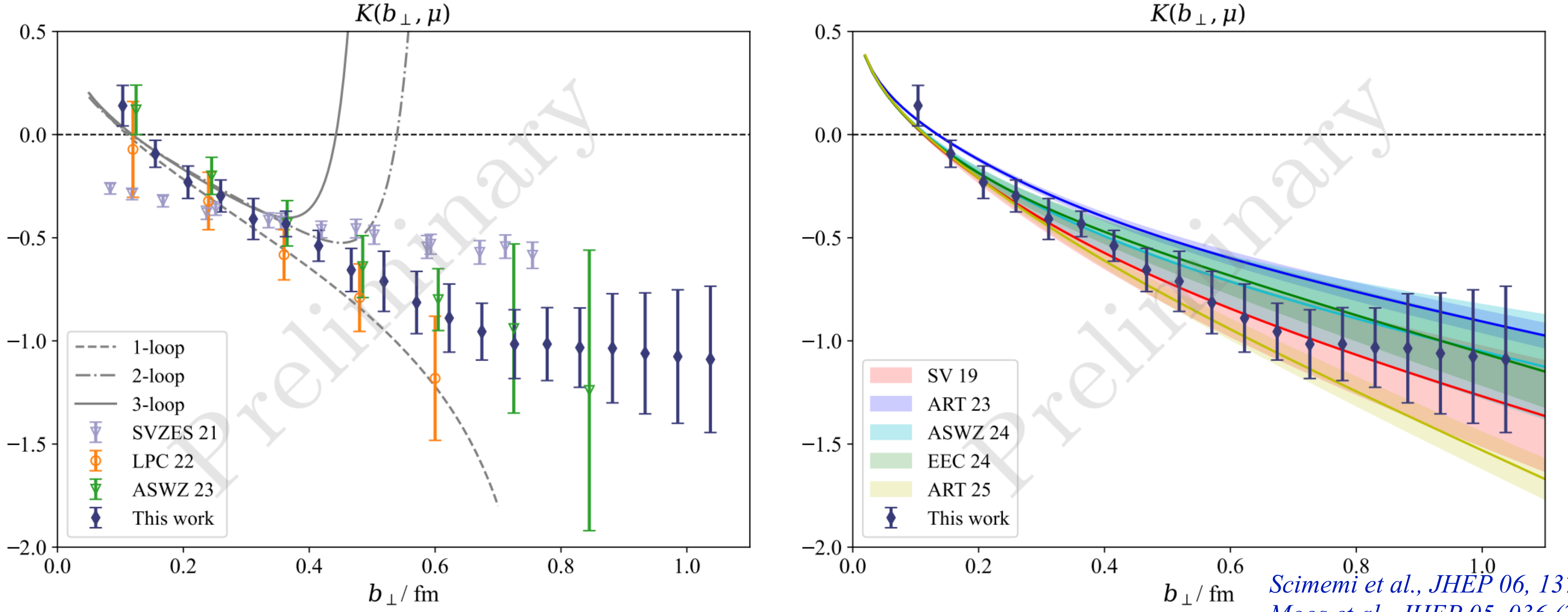

Schlemmer et al., JHEP 08, 004 (2021);
Chu et al. (LPC), PRD 106, 034509 (2022);
Avkhadiev, et al., PRD 108, 114505 (2023).

Scimemi et al., JHEP 06, 137 (2020);
Moos et al., JHEP 05, 036 (2024);
Avkhadiev et al., PRL. 132, 231901 (2024);
Kang et al., arXiv:2410.21435;
Moos et al., arXiv:2503.11201.

Review of CS Kernel Calculation

	Pion mass	Renormalization	Fourier transform	Matching	*x*-plateau	Continuum	separation (*)
SWZ20 PRD 102, 014511 (2020) Quenched	1.2 GeV	Yes	Yes	LO	Yes	No	0.8fm
LPC20 PRL 125,192001 (2020)	547 MeV	N/A	N/A	LO	N/A	No	0.3fm
SVZES JHEP08 (2021), 2302.06502	422 MeV	N/A	N/A	NLO	N/A	No	0.5fm
PKU/ETMC 21 PRL128, 062002 (2022)	827 MeV	N/A	N/A	LO	N/A	No	0.3fm
SWZ21 PRD 104,114502 (2022)	580 MeV	Yes	Yes	NLO	Yes	No	0.5fm
LPC22 PRD 106, 034509 (2022)	670 MeV	Yes	Yes	NLO	Yes	No	0.6fm
LPC23 JHEP 08,172 (2023)	220 MeV	Yes	Yes	NLO	Yes	No	0.6fm
ASWZ23 PRD108, 114505 (2023)	148.8 MeV	Yes	Yes	uNNLL	Yes	No	0.8fm
ASWZ24 PRL132, 231901 (2024)	148.8 MeV	Yes	Yes	uNNLL	Yes	Model (0.15,0.12,0.09) fm	0.9fm
LPC 25 (preliminary)	135.5 MeV	Yes	Yes	uNLO	Yes	Yes	~1.0fm

Table adapted/updated from Yong Zhao's collection

(*) Only the results that deviate from 0 by more than 2σ are considered.

Outline

➢ Motivation

➢ Lattice QCD calculation of Collins-Soper Kernel

- Quasi-TMD Wave Function
- Collins-Soper Kernel

➢ **Summary and Outlook**

Summary and Outlook

We present the lattice QCD calculation of CS kernel:

- ✓ **Systematic uncertainty have been carefully addressed;**
- ✓ **Physical extrapolation include large momentum, continuum limit and physical mass;**
- ✓ **The CS kernel has been extracted in the long-distance region ($b_\perp = 1\text{fm}$).**

In the future, we will:

- ➢ **Better control of uncertainties;**
- ➢ **Polarized TMDPDFs calculation;**
- ➢ **……**

Thank you for your attention!

Backup

TMDPDFs: 3D tomography of the nucleon

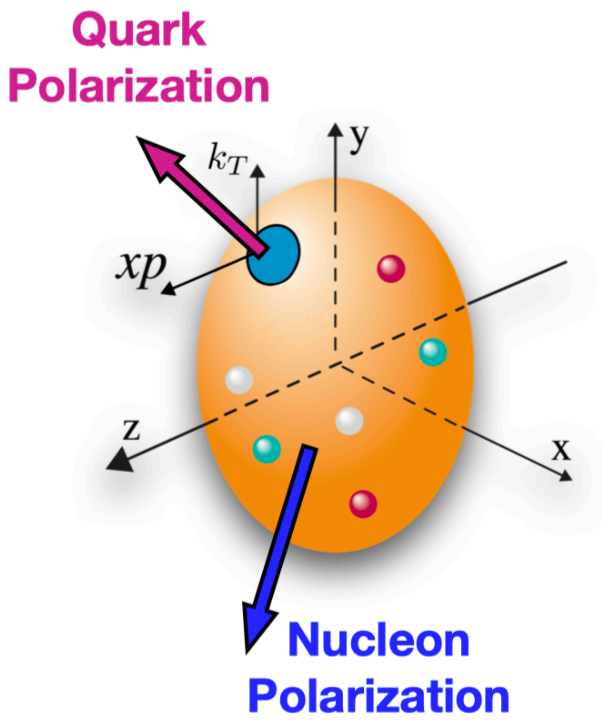

Leading Quark TMDPDFs

Nucleon Spin   Quark Spin

Nucleon Polarization	Quark Polarization: Un-Polarized (U)	Quark Polarization: Longitudinally Polarized (L)	Quark Polarization: Transversely Polarized (T)
U	f_1 = Unpolarized		$h_1^{\perp}$ = Boer-Mulders
L		g_{1L} = Helicity	$h_{1L}^{\perp}$ = Worm-gear
T	$f_{1T}^{\perp}$ = Sivers	$g_{1T}^{\perp}$ = Worm-gear	h_1 = Transversity; $h_{1T}^{\perp}$ = Pretzelosity

TMDPDFs are indispensable and multifaceted.

Boussarie et al., TMD Handbook, 2304.03302

Phenomenological vs. Lattice at TMD Observables

- The tensor charge δq is the first moment of the quark transversity distribution function $h_1(x)$:

$$\delta q = \int_0^1 dx[h_1^q(x) - h_1^{\bar{q}}(x)]$$

- There exists a noticeable difference between lattice QCD and phenomenological results obtained from global fits.

Most recent global data fit-Tensor Charge

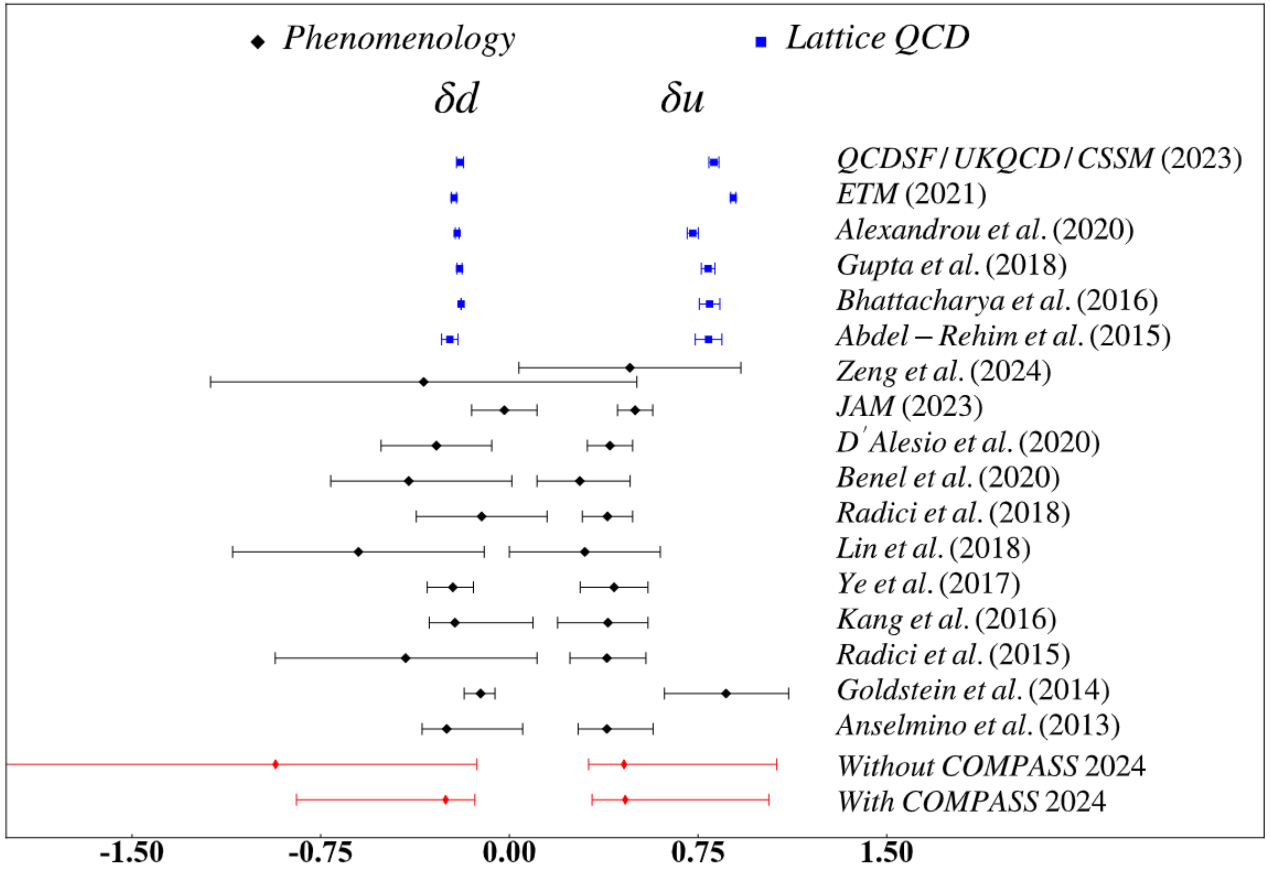

Zeng et al.,arXiv:2412.18324

High-precision calculations of TMDs on the lattice are urgently needed.

TMDs on Lattice QCD

- **Large-momentum effective theory: connecting Euclidean lattice and physical observables**

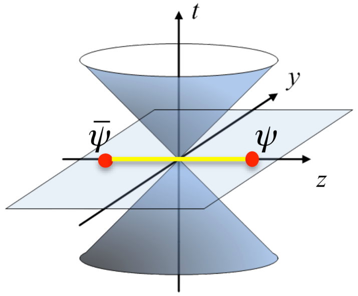

Lorentz boost

Ji, PRL110(2013), RMP93(2021), …

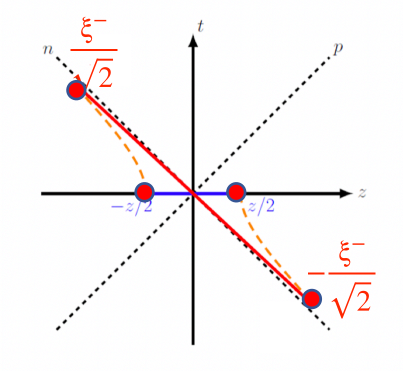

EFT

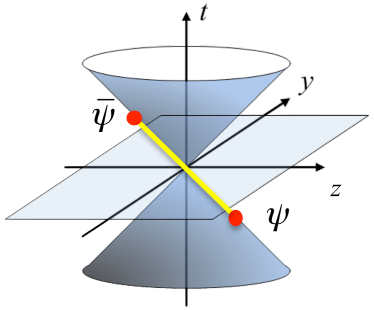

- **Achieved great success in the studies of TMDPDFs:**

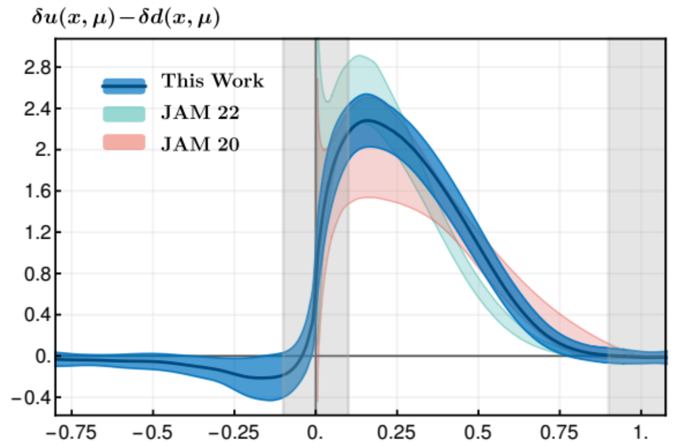

Proton transversity PDF, PRL131(2023)

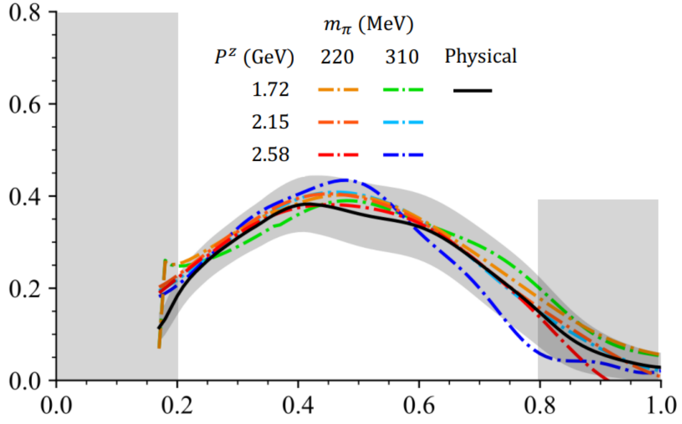

Unpolarized nucleon TMDPDF, PRD109 (2024)

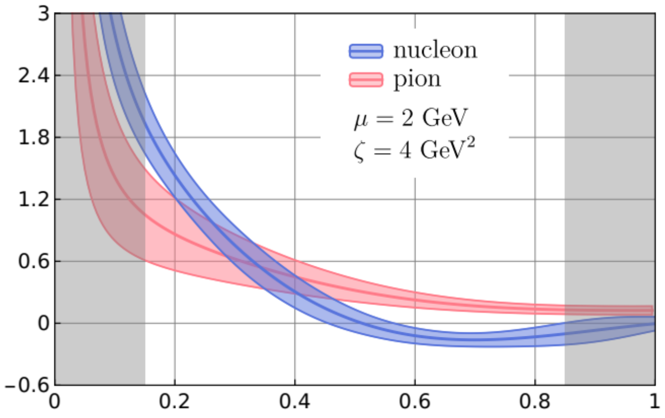

Boer-Mulders Function, arXiv:2502.11807

Dispersion Relation

➢ **We use the following fitting formula to fit the dispersion relation of pion,**

where the fit result is b1 = 1.0048 (90), b2 = -0.055 (16).

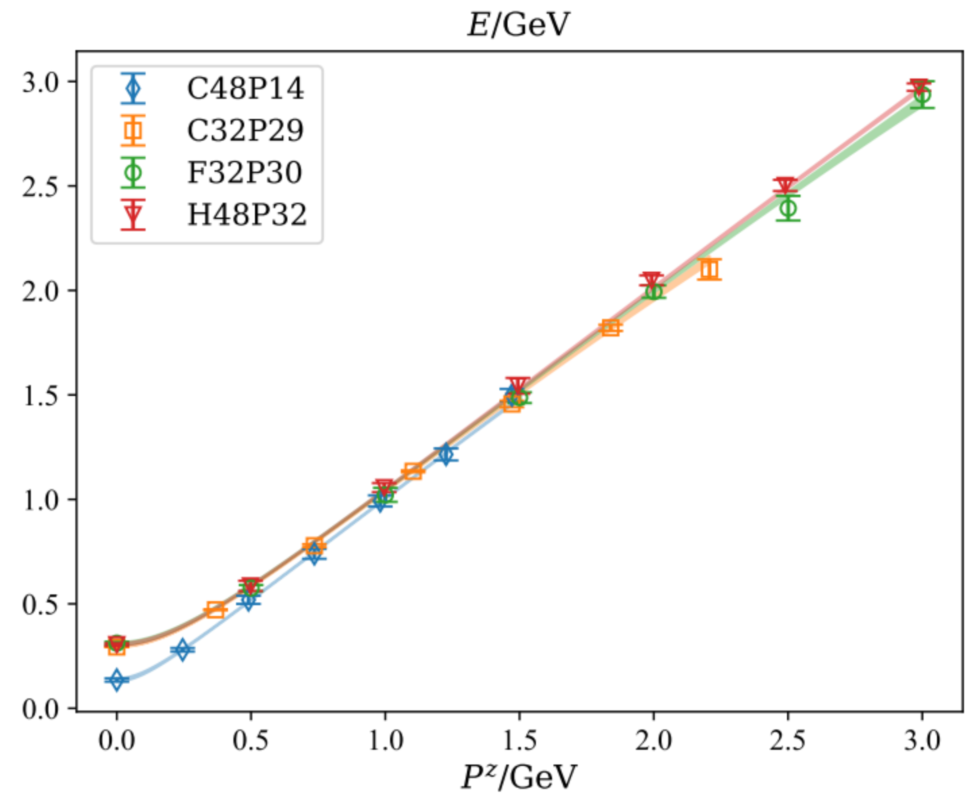

L Dependence

- ➢ **The extraction of $\tilde{\Psi}^{\pm}(x, b_{\perp}, \mu, \zeta_z)$ requires L to be large enough. When L ≥6a≅0.6fm, the matrix elements remain invariant.**

$$\tilde{\Psi}^{\pm}(x, b_{\perp}, \mu, \zeta^z) = \lim_{L\to\infty} \int \frac{dzP^z}{2\pi} e^{ixzP^z} \frac{\langle 0 | \bar{q}(z\hat{n}_z + b_{\perp}\hat{n}_{\perp}) \gamma^t \gamma_5 U_{c\pm} q(0) | \pi(P^z) \rangle}{\sqrt{Z_E(2L + |z|, b_{\perp}, \mu)} Z_O(1/a, \mu)}$$

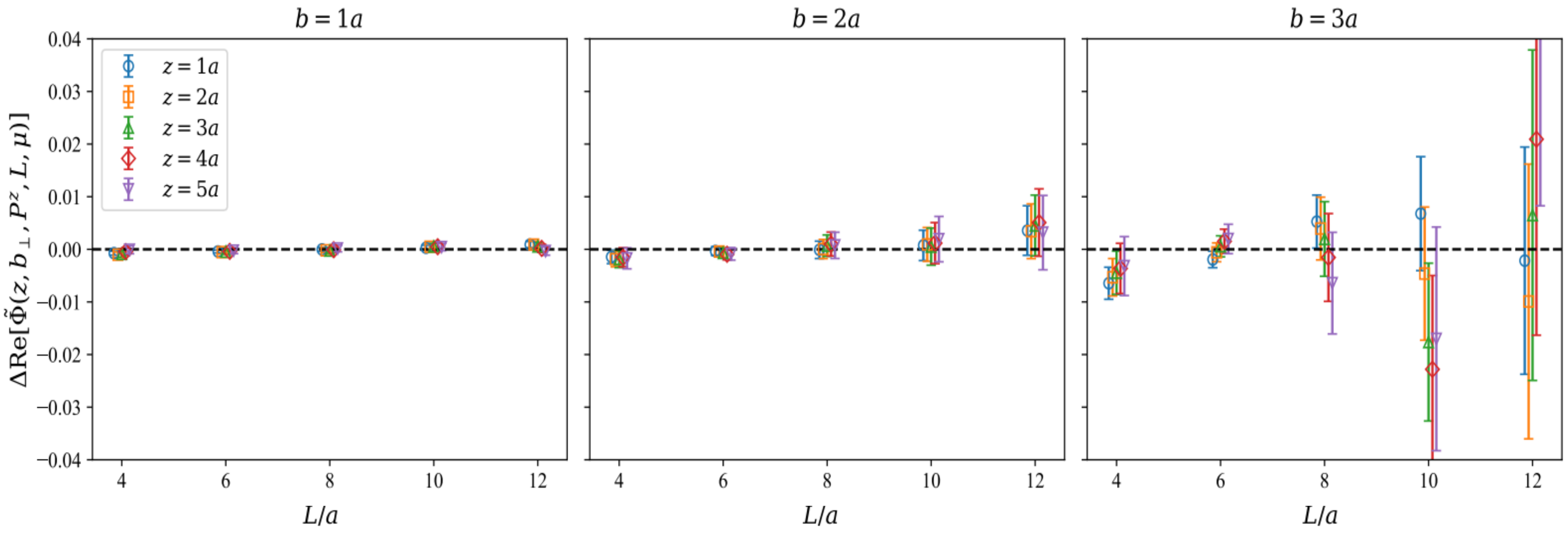

HYP smearing

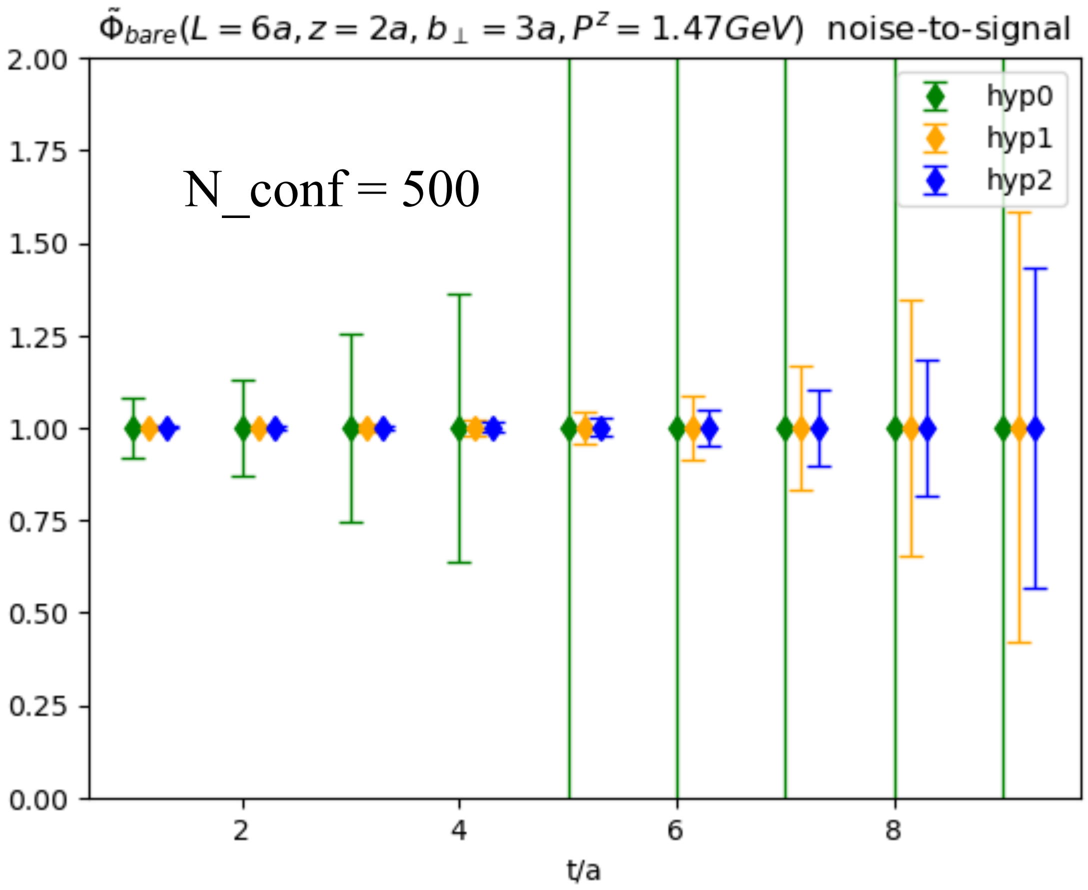

N_conf = 500, fix timeslice = 4a, Pz=1.47GeV, the noise-to-signal ratio of bare-TMDWF

$(b_\perp, z)$	HYP 0	HYP 1	HYP 2
(4,0)	0.5509	0.0187	0.0112
(4,3)	0.8883	0.1231	0.0706
(4,6)	2.0127	0.4808	0.1474
(4,9)	30.4924	0.5352	1.2179

- HYP smearing significantly suppress the noise-to-signal ratio of bare-TMDWF
- The noise-to-signal ratio of HYP smearing 1 times is lower than that of without HYP smearing.

“Imaginary part” of the CS kernel

➢ **The quasi-TMDWF factorization formula requires $xP^z b_\perp \gg 1,\ (1-x)P^z b_\perp \gg 1$, at small $b_\perp$ region, remain the dependence on $b_\perp$ when computing the matching kernel.**

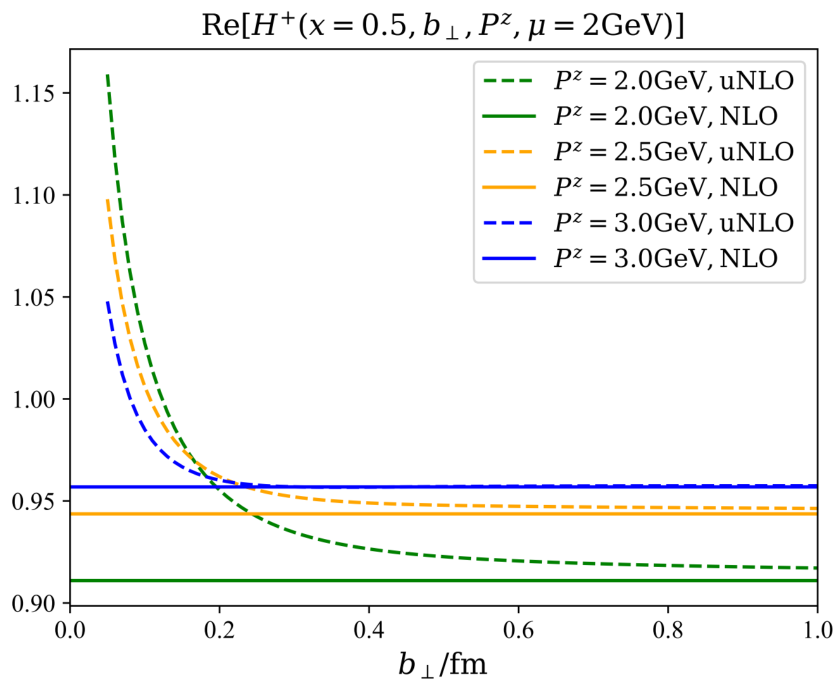

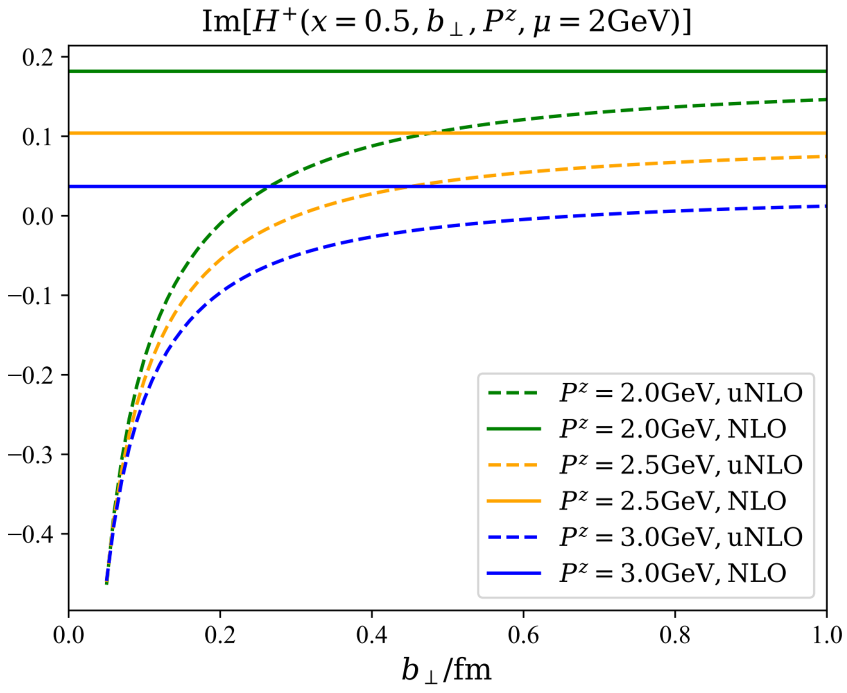

b-unexpanded matching kernel, PRD 108 (2023)

Different Lorentz Structures

When $P^z = 1.47\text{GeV}$

- $\Gamma_{src} = \gamma^t\gamma_5,\ \gamma^z\gamma_5, \gamma_5$ **are consistent when the timeslice is large;**
- **The signal-to-noise ratio of $\gamma^t\gamma_5,\ \gamma^z\gamma_5$ is greater than that of γ_5.**

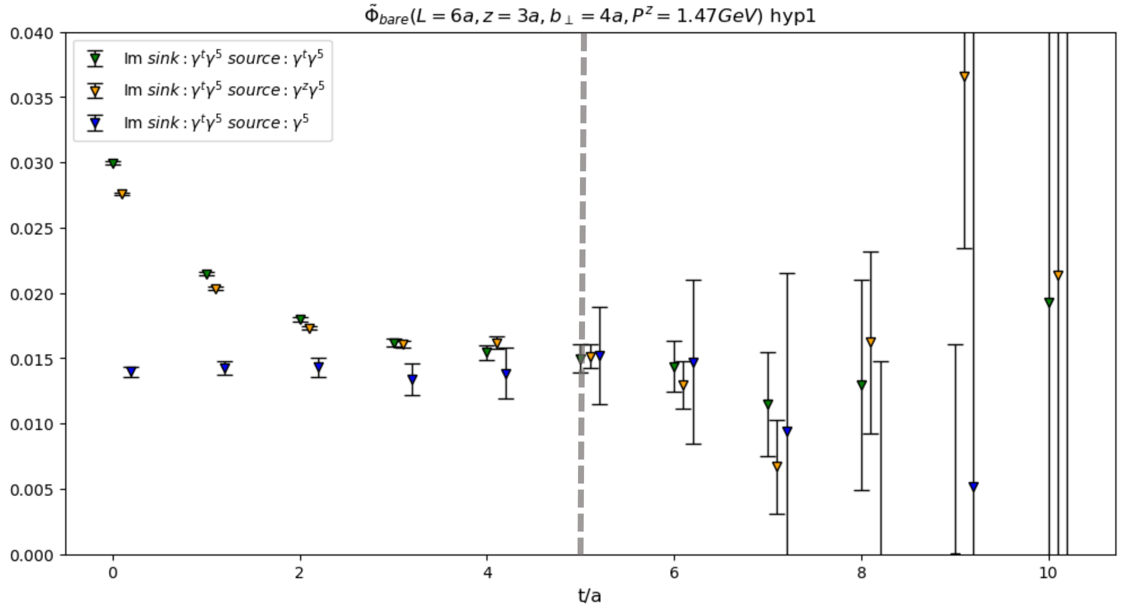

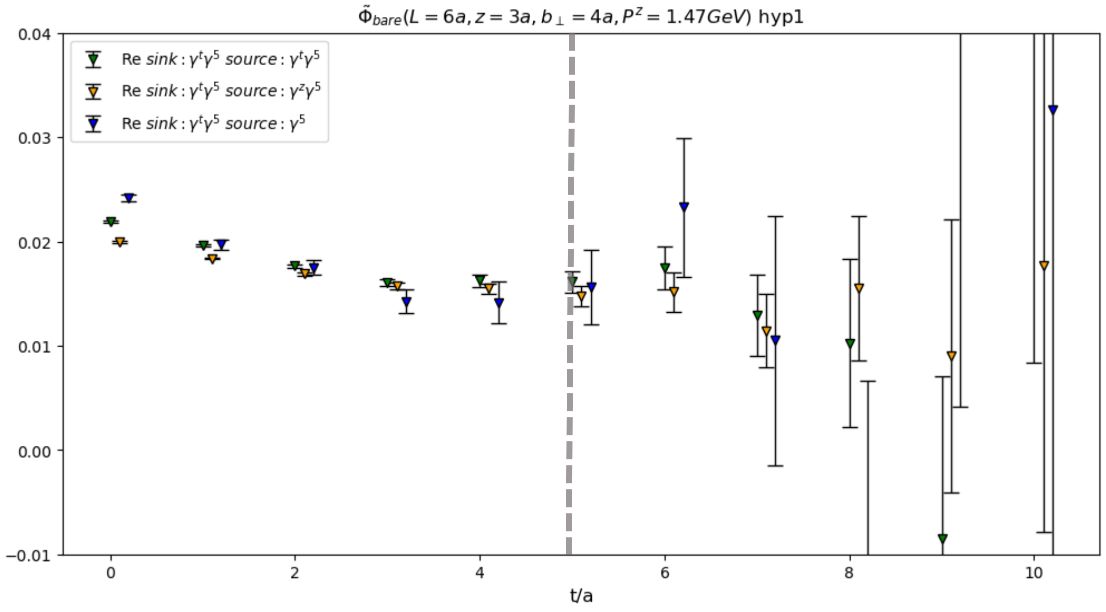

Gauge Fixing Accuracy and Lorentz Structure

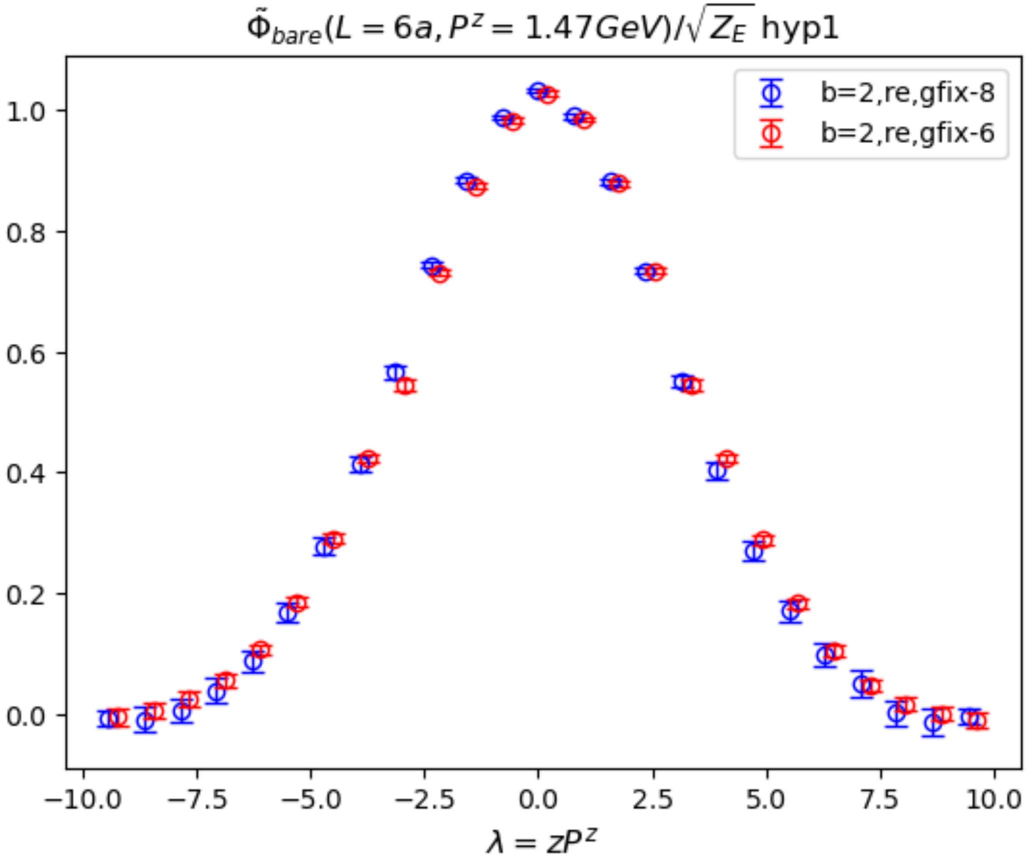

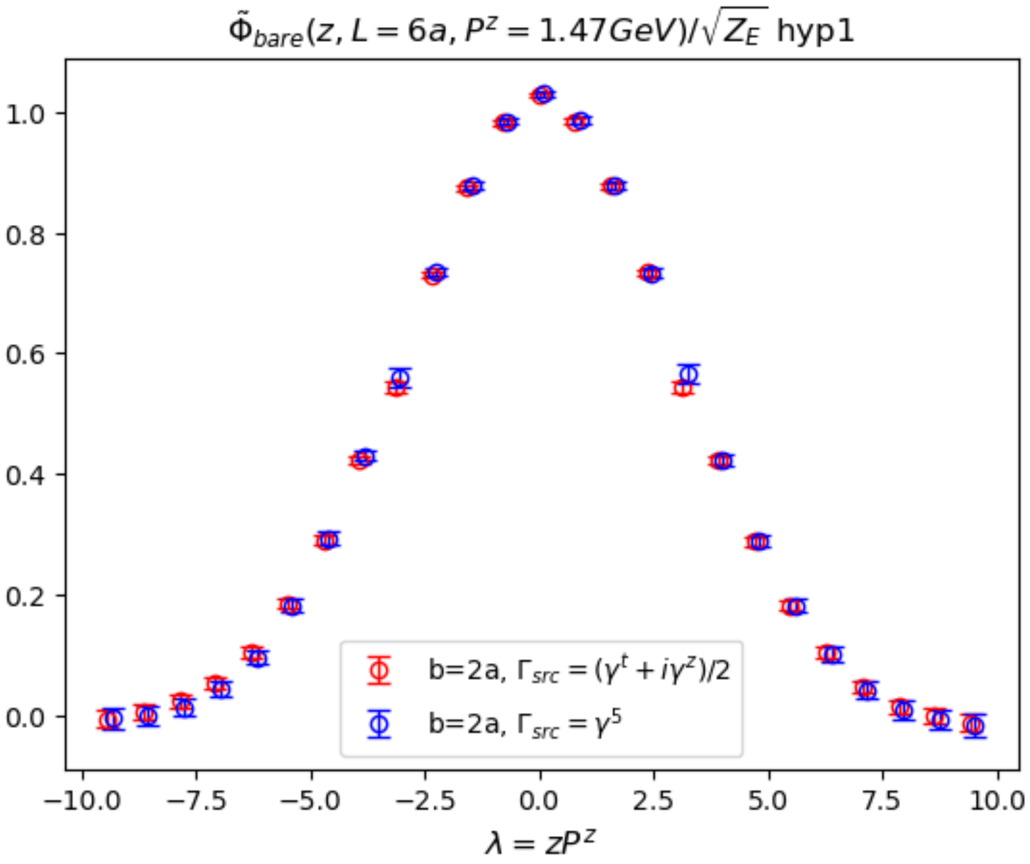

Left panel :

- the red: gauge fixing accuracy 10^{-6} ✓
- the blue: gauge fixing accuracy 10^{-8}

Right panel :We fix $\Gamma_{sink} = \gamma^t\gamma_5$,

- the red: $\Gamma_{src} = (\gamma^t\gamma_5 + i\,\gamma^z\gamma_5)/2$ ✓
- the blue: $\Gamma_{src} = \gamma_5$

Self-Renormalization--a New Scheme to Extract Z_O

Subtracted matrix element

- **Renormalization condition:** $\tilde{h}(a,z,b_\perp) = \frac{\tilde{\Phi}^0(z,b,Pz=0,\mu)}{\sqrt{Z_E(z+2L,b,\mu)}} = Z_O(1/a,\mu)h_0^{\overline{MS}}(\mu,b_\perp,z) + O(\frac{a^2}{b^2})$

- **Parametrization:**

$$\ln\tilde{h}(a,z,b_\perp) = \frac{\gamma_0}{\beta_0}\ln\left[\ln[1/(a\Lambda_{QCD})]\right] + \frac{c_1}{\ln[1/(a\Lambda_{QCD})]} + g(z,b_\perp)$$

$$\ln Z_O(a,\mu) = \frac{\gamma_0}{\beta_0}\ln\left[\ln[1/(a\Lambda_{QCD})]\right] + \frac{c_1}{\ln[1/(a\Lambda_{QCD})]} + d'(\mu)$$

Deng et al., JHEP 09 (2022); Huo et al. NPB 969(2021)

Self-Renormalization--a New Scheme to Extract Z_O

Subtracted matrix element

- **Renormalization condition:** $$\tilde{h}(a, z, b_\perp) = \frac{\tilde{\Phi}^0(z, b, Pz=0, \mu)}{\sqrt{Z_E(z+2L, b, \mu)}} = Z_O(1/a, \mu) h_0^{\overline{MS}}(\mu, b_\perp, z) + O(\frac{a^2}{b^2})$$

- **Parametrization:** $$\ln \tilde{h}(a, z, b_\perp) = \frac{\gamma_0}{\beta_0} \ln\left[\ln[1/(a\Lambda_{\rm QCD})]\right] + \frac{c_1}{\ln[1/(a\Lambda_{\rm QCD})]} + g(z, b_\perp)$$

Joint fit result： c_1=0.020

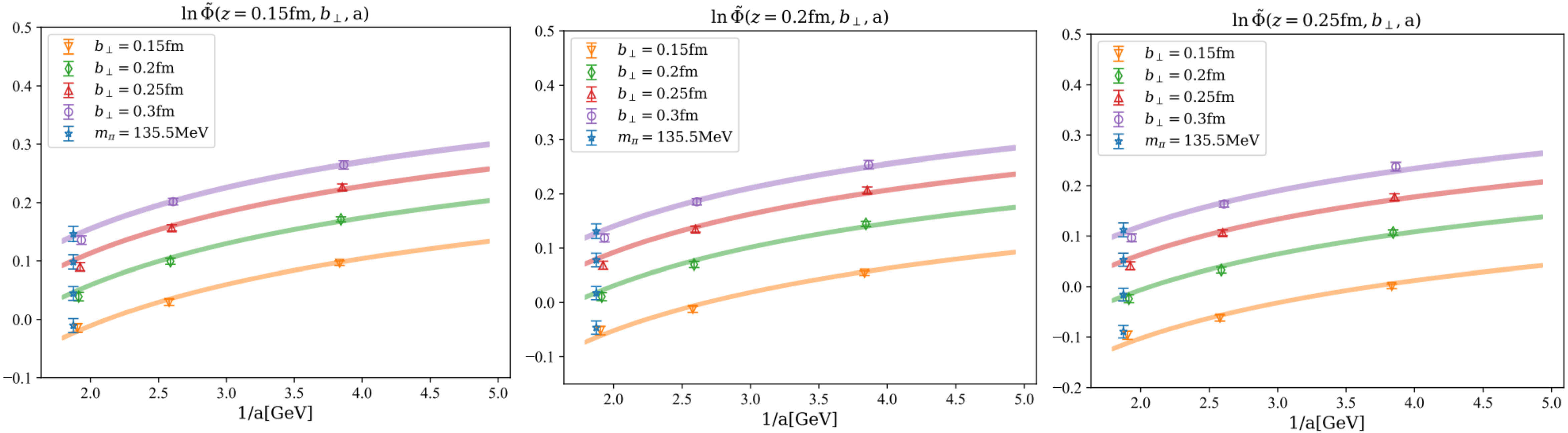

Deng et al., JHEP 09 (2022); Huo et al. NPB 969(2021)

Self-Renormalization--a New Scheme to Extract Z_O

Subtracted matrix element

- **Renormalization condition:** $\tilde{h}(a,z,b_\perp) = \frac{\tilde{\Phi}^0(z,b,Pz=0,\mu)}{\sqrt{Z_E(z+2L,b,\mu)}} = Z_O(1/a,\mu)h_0^{\overline{MS}}(\mu,b_\perp,z) + O(\frac{a^2}{b^2})$

- **Parametrization:**

$$\ln \tilde{h}(a,z,b_\perp) = \frac{\gamma_0}{\beta_0}\ln\left[\ln[1/(a\Lambda_{\rm QCD})]\right] + \frac{c_1}{\ln[1/(a\Lambda_{\rm QCD})]} + g(z,b_\perp)$$

$$\ln Z_O(a,\mu) = \frac{\gamma_0}{\beta_0}\ln\left[\ln[1/(a\Lambda_{\rm QCD})]\right] + \frac{c_1}{\ln[1/(a\Lambda_{\rm QCD})]} + d'(\mu)$$

Joint fit result： c_1=0.020

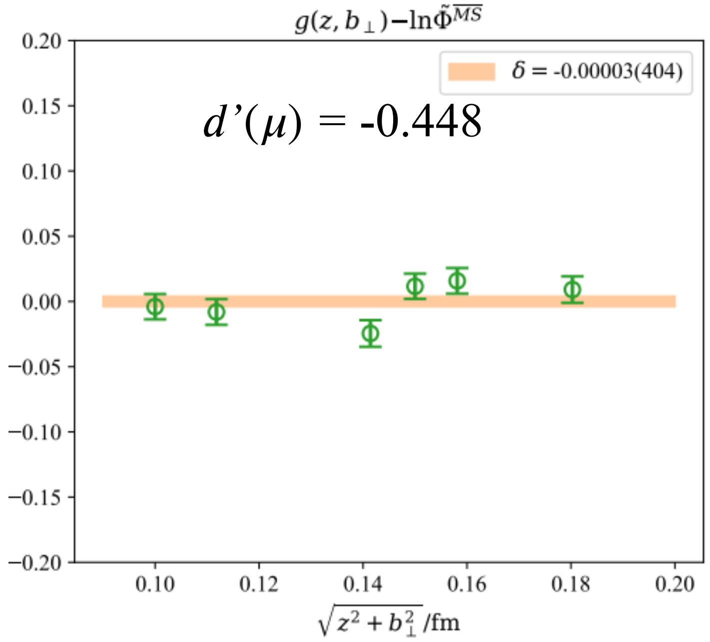

fm	0.10530	0.07746	0.05187
HYP0	1.064(21)	1.145(20)	1.241(19)
HYP1	0.92208(62)	0.97526(57)	1.03969(53)

Deng et al., JHEP 09 (2022); Huo et al. NPB 969(2021)